NCAR
Research Aviation Facility

Bulletin No. 24

AIRBORNE MEASUREMENTS FOR CLOUD MICROPHYSICS

rev. 1/89

Darrel Baumgardner

I. GENERAL

The Research Aviation Facility (RAF) provides airborne instrumentation for acquiring data in support of various facets of cloud microphysical research. These instruments measure the amount of cloud water, particle concentration, shapes, and sizes. Instrument configurations vary according to aircraft and scientific objective, and scientists who use data from these instruments should be aware of the measurement limitations imposed by the capabilities of the instruments and by particular mounting configurations, when applicable.

A. Cloud Particle Measurements

The accurate measurement of cloud particles is complicated by the large range of sizes, shapes, and concentrations found in the natural cloud types and conditions. In a cloudy environment, particle diameters may be as small as 10 cM, as in the case of cloud condensation nuclei, or larger than 1 cM, which is not unusual for graupel and aggregates of ice crystals. The concentrations of these particles range from > 1000 per cM^3 for the smaller sizes to < 0.1 per liter at the largest sizes. The particles may be spherical water droplets or complex dendritic ice crystals. The ability to analyze all of these types of particles, both quantitatively and qualitatively, requires more than a single instrument. The RAF presently has instrumentation capable of measuring particles over the range of 0.12 µM to > 6,400 µM in diameter by using combinations of particle probes that are manufactured by Particle Measuring Systems, Inc. (PMS, 1855 57th Street, Boulder, CO 80301). Aerosol particles ranging in size from 0.12 µM to 3.1 µM are sized and counted with the Active Scattering Aerosol Spectrometer Probe (ASASP). Water droplets from 0.5 µM to 45 µM in diameter are measured with the Forward Scattering Spectrometer Probe (FSSP). Water and/or ice particles ranging in diameter from 10 to 4,500 µM are sized and counted using one-dimensional (1D) optical array probes (OAPs). These OAPs thus overlap the FSSP in the cloud droplet range and extend to all but the largest sizes of hydrometeors usually encountered. If further differentiation between ice and water is desired, mixed-phase particles may be detected using the two-dimensional (2D) optical array probes for particles with

diameters ranging from 25 to > 6,400 μM. A summary of these probes, listing their size ranges and resolutions, is given in Table 1. Figure 1 illustrates the locations on each aircraft where the instruments are usually mounted.

B. **Cloud Liquid Water Content Measurements**

The amount of liquid water for a given volume of air may be determined through mass integration of the particle distributions measured by the PMS probes. Another method of directly measuring the liquid water content is with two different types of hot-wire probes (manufactured by Cloud Technology, 606 Wellsbury Ct., Palo Alto, California 94306 and PMS, Inc.). These instruments relate the change in resistance of a heated sensing wire to the amount of cooling caused by the vaporization of cloud droplets impinging on the sensors.

The liquid water content in supercooled clouds can also be estimated from the Rosemount icing rate detector described in the next section. Although liquid water estimates from this sensor are not as accurate as those from the hot wire probes, much lower liquid water contents can be detected. The ice probe is especially useful in mixed phase clouds where measurements from other methods of detection are affected by ice particles.

C. **Cloud Icing Measurements**

The icing rate in supercooled clouds can be estimated through the use of the previously-described instruments and their measurement of droplet size and liquid water content. As a direct measurement of icing rate, the RAF uses a Model 871 icing detector manufactured by the Rosemount Engineering Co., P.O. Box 35129, Minneapolis, Minnesota 55435. This probe produces a voltage proportional to the ice accumulated on a cylinder which is exposed to supercooled water droplets in the airstream.

D. **Particle Spatial Distribution Measurements**

Small-scale structure of cloud particle distributions are measured using the particle spacing monitor (PSM) developed at RAF. By measuring the arrival times between individual particles detected by either the FSSP or 1D OAPs, the spacing between particles is measured directly. The 2D OAPs also provide the interarrival times of particles which they image.

E. **Further Information**

Note: Separate from this Bulletin, the following hyperlinks have newer, additional information on the instruments described here.

From Darrel Baumgardner:

- Passive Cavity Aerosol Spectrometer Probe
- Forward Scattering Spectrometer Probe Model-100
- Forward Scattering Spectrometer Probe Model-300
- 1D Optical Array Probe
- 2D Optical Array Probe
- Liquid Water Probe

Rosemount Icing Probe

From Chris Webster:

- PMS-2D Probe Description

II. THE ACTIVE SCATTERING AEROSOL and FORWARD SCATTERING SPECTROMETER PROBES

A. Operating Principles

The ASASP and FSSP relate the amount of forward-scattered light by a spherical particle to its size according to electro-magnetic-wave scattered light by a spherical particle to its size according to electro-magnetic-wave scattering theory. The ASASP uses an aerodynamically-focused airstream to define a fixed sample volume (Figure 2.) The FSSP uses two photodetectors to define the sample volume in which the particles will be detected. One photodetector is optically masked so only the light outside the defined depth-of-field (DOF) is detected. The signal from this detector is used to discriminate particles outside the DOF (Figure 3.) The source of illumination is a He-Ne laser operating at wavelength of 6328 angstroms. All the optics and electronics are integrally packaged with the exception of the data system required to store the accumulated size and concentration information.

B. Calibration Procedures

The ASASP and FSSP are calibrated periodically before and after each field project to check for sizing accuracy. Monodispersed glass beads are used to determine the necessary sizing information with appropriate corrections made for the index of refraction differences between glass and water. The laser beam diameter and DOF also are checked periodically to maintain an accurate record of the sample volume of the FSSP. The flow rate through the ASASP, which is a constant-volume device, also is routinely checked.

C. Probe Limitations

Cloud particle concentrations measured by these probes are under-estimated when particles are either coincident in the beam or pass through the sensing area of the probe during the electronic processing period of a previously-detected particle. The combination of these effects typically exceeds 10% when the natural particle concentrations are greater than 300 per cM^3. The majority of these losses, however, may be recovered as described by Baumgardner, et al. (1985).

The sizing accuracy is affected by several factors. Although the lasers used in the probes are operated in a higher-order mode to produce a semi-uniform beam intensity, there are still significant non-uniformitites which affect the amount of light that a particle scatters. This problem is compounded by the response time of the electronics that causes particles to be undersized at airspeeds greater than about 50 M/s. Corrections are applied to the data that account for this problem (Baumgardner, 1987). Mis-sizing also will occur as a result of particles coincident in the beam which will be detected as a single particle but sized somewhat larger. This type of sizing error will usually be negligible, and, at present, no attempt is made to correct the data for this event. However, special software is available from RAF that can be used when special

processing is desired by the user.

Another limitation implied in the principles of operation is that these probes cannot discriminate between water and ice particles. Ice particles pass through the sample volume of these probes in random orientation, and the measured sizes will depend upon this orientation and the shape of the crystals. Ice particles outside the nominal sample area of these probes will sometimes be sized and counted if they fall partially within the sample volume. Therefore, the sample volume for ice particles will be indeterminate. For these reasons, the FSSP or ASASP should not be used for ice crystal measurements, and measurements from these probes should be used carefully whenever they are used in known mixed-phase situations. In these conditions, the spectra usually show a characteristic flat shape in the larger size channels.

III. THE ONE-DIMENSIONAL OPTICAL ARRAY PROBE

A. Operating Principles

The 1D illuminates a linear array of photodiodes with a He-Ne laser. As a particle passes through this focused beam, a shadow image is cast on the diodes (See Figure 4.) and a count of the total number of occulted diodes represents the particle's size. The diodes at each end of the array act as a mechanism for rejecting those particles which do not pass entirely within the bounds of the linear array and would be undersized otherwise. The 1D probe types are differentiated by their magnification factors according to the size range desired. The 200X sizes particles with diameters from 40 µM to 280 µM in 20 µM increments; the 200Y sizes particles from 300 µM to 4,500 µM in 300 µM increments; and the 260X sizes particles from 40 µM to 620 µM in 10 µM increments.

B. Calibration Procedures

The 1D probes are calibrated periodically before and after each field project. The imaging probes are quite stable in their sizing of particles, and changes occur only because of changes in optical path or exceptionally dirty optical components. The sizing calibration is done with monodispersed particles, such as glass or polystyrene beads. These particles are projected across the DOF until a statistically suitable number of counts have been accumulated. Routine maintenance is a part of RAF procedures for insuring the integrity of the measurements. Such maintenance includes checking laser alignment and cleaning dirty optical elements.

C. Probe Limitations

The electronic response time of the instruments imposes some limitation on the minimum detectable size. A photodiode is registered as shadowed when its output is detected to change by 50%. However, even when a particle shadows 50% of a diode, the detected change may be less than this size if the particle passes too rapidly across the array. This condition depends upon the size of the particle as well as the width of the array. The 200X and 260X have lower size limits of 40 µM at a speed of 100 M/s because of this effect.

Although the 1D probes will detect any particles which cause the diode array to be occulted, these probes cannot differentiate shapes, types, or particle orientation. If liquid water content information is desired, some fairly loose assumptions must be

made with regards to the phase, habit, and density of the particles. These assumptions can lead to non-trivial errors.

The 1D probes are unable to resolve particles coincident in the beam; however, this type of error can usually be neglected, since concentrations of particles of the size measured by these instruments are normally quite small.

Obtaining a statistically representative sample of the cloud particle population can also be a problem because of the relatively small sample volume of these instruments and the small concentrations of larger particles in a cloud. The sample volume of these probes is size dependent. Appendix A discusses how to calculate these sample volumes.

IV. THE TWO-DIMENSIONAL OPTICAL ARRAY PROBE

A. Operating Principles

The 2D OAP's optical detection system is almost identical to that of the 1D probe. Whereas the 1D probes only give information about the maximum dimension along the array width, the 2Ds also give information about the area and shape of the particle and don't reject particles that shadow end elements. As a particle passes through the 2D's DOF and occults the diodes in the array, the shadowed state of each diode is stored each time the probe moves the distance of one array width. These image slices are restored during analysis later to form a reconstructed two-dimensional image of each particle. This method of measurement allows the shape of the particle to be discerned as well its size. Some information concerning the composition of the particle may be deduced from the shape and from other information such as the temperature, liquid water content, or altitude at which the aircraft made its measurements. The 2Ds are classified as either a 2D-C (cloud particle probe), which detects particles with diameters from 50 µM to > 800 µM in 25 µM intervals, or as a 2D-P (precipitation probe), which detects particles with diameters from 200 µM to > 6,400 µM in 200 µM intervals.

A 2D probe also sends to the data system a "Shadow-Or" count, which is generated every time a particle passes through the laser. The image data are stored by the data system asynchronously and require separate processing from the synchronous data from other sensors. However, the Shadow-Or count is accumulated at the same rate as the rest of the synchronous data and can be used to calculate estimates of particle concentrations.

B. Calibration Procedures

The 2D probes are calibrated and aligned with the same procedures and regularity as the 1D probes.

C. Probe Limitations

One limitation arises from the large quantity of information produced by the 2Ds which is necessary for the two-dimensional description of a particle. If the 2D probe is operated at its maximum sampling rate, a typical 7-inch reel of magnetic tape will be filled in about five minutes or about the same time as it would take to make a single cloud pass. The maximum rate at which the 2D probe can store image slices is 4 million slices per second. This rate will not impose airspeed limitations on the lower-

resolution probes. However, for the 25 µM resolution 2D-C probe, this will mean that images will become distorted at airspeeds greater than 100 M/s. When the airspeed exceeds 100 M/s, the slice rate is maintained at the maximum rate. This causes shortened images along the direction of flight.

The high sampling rate of the 2D probe will sometimes impose another limitation on particle measurements. The image slices are stored temporarily in buffers in the probe. After one buffer is filled with 1,024 image slices, it is transferred to the data system while a second buffer is being filled. Although the image data may be collected at a rate up to 4 million slices per second, they can only be transferred to the data system at about 30k slices per second. This poses a problem only during episodes of high ice concentration. During these periods, the second buffer can become filled before the first buffer has finished emptying to the data system. This condition is called an "overload," and simply means that the probe is unable to take data during these periods.

The orientation of ice crystals can be affected by air distortions caused by the aircraft. Measurements at the mounting locations of the PMS proves on the King Air (See (Figure 1.) are particularly susceptible to these effects because of sheared flow in front of the probe. Crystals such as plates and dendrites have been observed to rotate into preferred orientations that will cause them to be viewed on edge if the orientation of the probes is not adjusted to account for these rotations. The 1D and 2D probes are flown in an orientation to minimize these effects; however, the image data should be viewed with discretion.

D. Data Reduction

During the flight, the 2D images may be displayed on a CRT, but no hard copy is currently available. After the project the 2D data are processed by programs that eliminate spurious particles, plot the images on microfilm, and print derived values of concentration and size distributions. Appendix D provides a more complete description of the criteria used for detecting and eliminating spurious particles.

Interpretation of the 2D images is highly subjective. For this reason, the RAF does not process the image data with any automatic pattern-recognition software and leaves that option to the user.

E. Further Information

Additional information on the PMS-2D probes can be found at
http://www.atd.ucar.edu/atd/instruments/raf/pms2d/

V. THE PARTICLE SPACING MONITOR

A. Operating Principles

The particle spacing monitor (PSM) provides a measurement of the small-scale structure of cloud particle distributions by measuring the spacing between individual particles. This instrument monitors the total particle count from an FSSP or 1D probe and measures the time between successive counts. This time is encoded into one of 64 size channels and sent to the data system in the same manner as particle size data from other 1D probes. The time-to-channel relationship can be set to any desired value,

depending upon the expected distribution of the cloud particles. Figure 5a is a schematic representations of the PSM. Figure 5b is an example of the type of distribution produced by this instrument.

B. Limitations

The PSM is limited only by the probe to which it is attached. For example, when attached to the FSSP, the minimum spacing between particles that the PSM can measure is slightly greater than the combined transit time of a particle through the laser and the subsequent electronic delay time. This is usually on the order of 7-8 µs, or a spacing of 0.7-0.8 mM if the aircraft is flying at 100 M/s.

VI. THE CLOUD TECHNOLOGY AND PMS/CSIRO PROBES

A. Operating Principles

The operating principle of these two instruments (commonly referred to as the JW and KING probes, respectively) are based upon measuring the amount of cooling of a heated sensor by the evaporation of water droplets as they impact the sensor. These devices, shown schematically in Figures 6a and 6b, differ in their methods of measuring the amount of cooling. The JW senses changes in the resistance of the heated element as it cools, and through calibration, relates it to the liquid water content. Cooling is also caused by convective heat losses, so the probe measures these losses with a second heated wire oriented to be out of the droplet stream but still in a component of the airstream. This "compensation" signal is subtracted electronically from the sensing wire signal so that the resultant measurement is only of the liquid water component of cooling. The KING probe operates as a constant-temperature probe and measures the amount of power necessary to maintain the heated element at the same temperature while it is cooled by convection and evaporation. The liquid water content can be directly related to the power consumption using the energy equation that relates the total energy supplied to the sensing element to the energy lost through convection and evaporation. Convective heat losses are determined through calibration in dry air over a range of air speeds and temperatures.

B. Calibration Procedures

The JW probe requires wind tunnel calibrations to establish the gain coefficients for each individual sensing head. The compensation-wire offset is adjusted during speed runs at different altitudes prior to the beginning of a field program.

The KING probe requires no calibration for translating the power loss to liquid water content, as this is determined from the energy balance equation. (See Appendix C.) The convective heat losses must be determined, however, since they are affected by the environmental conditions, e.g., air density, viscosity, thermal conductivity, etc., and the wire dimensions and temperature. The dry air heat loss term also is explained in Appendix C.

C. Probe Limitations

The JW probe is sensitive to liquid water content values down to approximately 0.05 g/M^3, below which the inherent noise of the instrument masks any signal. The dry air compensation wire does not adequately remove all the effects of convective heat losses.

This limitation is seen when the out-of-cloud measurements vary as much as 0.1 g/M^3. These drifts are removed during data processing when possible. (See Appendix C.)

As a device for measuring relative changes in the liquid water content, the JW has proved fairly reliable under a wide range of conditions. However, its accuracy as an absolute measure of liquid water content is questionable without measuring its response in a calibrated wind tunnel. Such calibrations have proved to be the best method of determining JW probe reliability and calibration. Extensive testing has shown that the response of this probe differs with each sensing element. Without a careful calibration, the accuracy of these probes is no better than approximately 20%.

Under particularly severe conditions where the liquid water content is greater than 1.0 g/M^3 and the temperature is below -15C, the heaters in the JW sensing head are not sufficient to melt quickly enough any ice that has accumulated on the probe shield. Subsequently, ice builds up on the compensation wire, and erroneous data are obtained.

When droplet diameters exceed about 30 μM, droplets begin to break up on the sensing elements of both the JW and KING probes and are removed by the airflow before they have totally evaporated. Under these circumstances, both probes will underestimate the liquid water content.

Both the JW and KING probes respond to ice particles as well as water droplets. However, these probes are not calibrated with respect to ice, and caution should be used when interpreting data from these probes in mixed-phased environments.

The KING probe is considered by the RAF to be the primary instrument for measuring liquid water content because of its reliability and easy calibration. The JW is flown as a redundant measurement should there be a failure of the KING probe.

D. Data Reduction

Processing of the data from these probes includes corrections for airspeed on the JW and dry-air heat losses on the KING probe.

VII. THE ROSEMOUNT ICING DETECTOR

A. Operating Principles

The Rosemount Model 871 detector, shown schematically in Figure 7, measures the amount of ice mass accumulation on a metal cylinder. The property of certain metals known as magnetostriction is employed to drive the sensing probe cylinder at its natural frequency of 40 kHz. As the ice accretes on the cylinder, the frequency of the vibration decreases. A phase-locked loop detects the change in frequency, and a voltage proportional to this change is recorded by the data system. When a preset voltage threshold is reached, the probe tip is heated for a fixed, short period of time to remove the ice, whereupon the cycle is repeated. This probe is primarily an icing detector; however, with additional information about the temperature and air speed, an ice water content can be estimated from its measurements.

B. Calibrations

The frequency change versus mass relationship is known through both theoretical and

empirical studies. Wind tunnel tests have been conducted in which the operation of this probe was studied during typical airspeeds and icing conditions to establish the gain coefficients of the instrument. Flight data also are used to determine the calibration coefficients that are used to calculate the ice water content from these probes. The liquid water content is derived from the equations described in Appendix C.

C. Limitations

The ice probe is a very sensitive device and responds to very small ice water contents. Data loss occurs, however, during the deicing period and for about a five-second period after this, as the probe reaches equilibrium with the ambient temperature.

Ice water contents derived from the icing rate measurements have an uncertainty on the order of 20% as a result of uncertainties in droplet collection efficiency and sampling volume.

VIII. FURTHER INFORMATION

Investigators interested in discussing additional aspects of cloud physical measurement should contact the Facility Manager, Jeffrey L. Stith, PhD

email
Phone: (303) 497-1032

Additional information on the instrumentation discussed above may be found in the Bibliography listed at the end of this Bulletin.

APPENDIX A.

Calculation of Particle Spectrum Parameters

The particle distributions measured by the ASASP, FSSP, 1D, and 2D are usually characterized by the total concentration, the mean diameter, the standard deviation, and the liquid water content. An explanation and derivation of these parameters follow.

Total Concentration

Particle concentration is defined as the number of particles per unit volume. In the case of the ASASP and FSSP, the dimensions are the number of particles per cubic centimeter. Concentrations measured by the imaging probes are usually expressed in number per liter. The method of calculating the total concentration is:

$$C_T = \frac{\Sigma_{i=1}^{m} n_i}{SV}$$

(A.1)

where:

c_T = total concentration
n_i = number of particles accumulated in channel ***i*** (for all probes but the FSSP)
Σn_i = total droplets passing through the ***DOF*** for the FSSP
m = total number of size channels
SV = sample volume

The sample volume is defined as:

$$SV = (TAS)(SA)(T)$$

(A.2)

where:

TAS = true airspeed
SA = sample area
T = sampling period

The sample volume is determined for the FSSP by:

$$SA = (DOF)(BD)$$

(A.3)

and for the imaging probes by:

$$SA = (DOF)(ESW)$$

(A.4)

where:

DOF = depth of field
BD = effective beam diameter
ESW = effective sample width

The ASASP is a constant-volume device and is set to 1.0 cM^3/s. The DOF and ESW of the imaging probes are functions of the particle size and are calculated as (Knollenberg, 1970):

$$DOF = \frac{6R^2}{\lambda}$$

(A.5)

where:

R = radius of the particle (mM)
λ = laser wavelength = 0.6238 x 10^{-3} mM

which gives a DOF of

$$DOF = 9482\ R^2 \tag{A.6}$$

The DOF of the instruments is limited by the distance between probe arm tips. The maximum depth of field for the 200X, 260X, and 2D-C is 61 mM, which corresponds to a particle radius of 80 µM. The 200Y and 2D-P have a maximum depth of field of 261 mM for particles 165 µM radius or larger.

The effective sample width for the 1D probe is defined as:

$$ESW = \frac{D(N - X - 1)}{M} \tag{A.7}$$

where:

D = diode diameter = 0.2 mM
M = probe magnification factor
N = number of diodes in the array
X = number of diodes shadowed by a particle

This method of determining the effective sample width is used to account for the fact that, as particles get larger, the probability increases that they will occult an end diode and be rejected. Table A.1 tabulates M, N, and sample area formulae for each of the 1D imaging probes.

TABLE A.1

PROBE TYPE	Magnification M	DIODES In ARRAY N	SAMPLE AREA EQUATION (mM^2)
200X	10	16	189.6 x (15 - X) x R^2 (R <= 80 µM) 1.22 x (15 - X) (R > 80 µM)
260X	20	64	94.8 x (63 - X) x R^2 (R < 95 µM) 0.86 x (63 - X) (R >= 95 µM)
200Y	0.667	24	284.30 x (23 - X) x R^2 (R < 175 µM) 87.3 x (23 - X) (R >= 175 µM)

The ESW of the 2D probes is determined in a different fashion than that for the 1D probes, since particles which shadow the end diodes are not rejected and can be included in the sample statistics if the sample volume is adjusted accordingly. A particle-weighting technique is used which increases the ESW with increasing particle size. Figures A.1 and A.2 show the sampling areas for the five probes as a function of particle diameter.

Mean Diameter and Standard Deviation

The mean diameter is the arithmetic average of all particle diameters and is calculated by:

$$\overline{D} = \frac{\Sigma_{i=1}^{m} n_i d_i}{N_T}$$

(A.8)

The standard deviation is a measure of the deviations from the mean and is calculated by:

$$S = \left(\frac{\Sigma_{i=1}^{m} n_i d_i^2}{N_T} - \overline{D}^2\right)^{1/2}$$

(A.9)

where:

$\overline{D}$ = mean diameter (μM)
S = standard deviation (μM)
N_i = number of particles in channel ***i***
d_i = size of which channel ***i*** represents (μM)
m = number of channels
N_T = total number of particles

Liquid/Ice Water Content

The liquid or ice water content is calculated from the measured size spectrum using a summation of the individual particle masses per unit sample volume:

$$LWC/IWC = \rho_w \Sigma_{i=1}^{m} N_i d_{ie}^3$$

(A.10)

where:

ρ_w = density of water
N_i = concentration of particles in size channel ***i***
d_{ie} = equivalent melted diameter (the size an ice particle would be if it were melted) in size channel ***i***

The equivalent melted diameter is strongly dependent upon the particle habit which is measured. The method for choosing this value must be specified by the user.

Radar Reflectivity

The radar reflectivity is defined as the amount of reflectivity a measured distribution of particles would have If detected by a radar. This reflectivity is calculated with dimensions of decibels (dBZ) and is dependent upon the wavelength of the radar and the density of the particles. This reflectivity is calculated as follows:

$$dB(Z) = \log_{10}(\Sigma_{i=1}^{m} N_i d_{ie}^6)$$

(A.11)

where:

dB(Z) = decibels of reflectivity
N_i = concentration of particles in size channel ***i***
d_{ie} = equivalent melted diameter (the size an ice particle would be if it were melted) in size channel ***i***

APPENDIX B.

FSSP Sample Area Calculations and Dead Time-Coincidence Corrections

Sample Area Calculations

The sample area of the FSSP is just its depth of field times the effective beam diameter. The effective beam diameter is some fraction of the total diameter that is dependent upon the velocity averaging mechanism of the instrument used to exclude particles passing through the edges of the beam. A running average of each particles transit time through the beam is maintained electronically. Each incoming particles transit time is compared to the average. If the particles time is less than the average, it is rejected from sizing but still included in the running average.

The ratio of accepted particles to all particles used in the average is a measure which may be employed to determine the fraction of the sample area to use in concentration calculations. Therefore, the FSSP sample area is calculated by

$$SA = \frac{(DOF)(BD)n_a}{n_t}$$

(B.1)

where:

DOF = depth of field
BD = beam diameter
n_a = velocity-accepted particles
n_t = total particles passing within ***DOF*** (total strobes)

Coincidence and Deadtime Corrections

The correction for particles missed because of coincidence in the beam or because of passage through the beam during the electronic dead time involves an extensive statistical analysis beyond

the scope of this bulletin. Only the end results with the necessary definitions will be given. Details of the derivations and accompanying assumptions may be found in Baumgardner et al. (1985). In short, the total number of particles passing through a scattering probe's sample volume during a given sample time can be expressed as

$$n_a = n_m + n_c + n_d \tag{B.2}$$

where:

n_a = actual number of particles passing through the DOE
n_m = measured number of particles passing through the DOE
n_c = particles undetected because of coincidence during the sampling period
n_d = particles undetected because of dead time during the sampling period

The coincident particles lost, n_c, are estimated using Poisson statistics, such that

$$n_c = n_a(1 - e^{-\lambda\tau_1})(1 - P_d) \tag{B.3}$$

where:

τ_1 = average transit time of a particle through the laser beam
λ = mean arrival rate of a particle in the beam
P_d = probability of a dead time event occurring

The average transit time is found by

$$\tau_1 = 0.78W/v \tag{B.4}$$

The mean arrival rate is given as

$$\lambda = N_a W v (L_D + 2L_1) \tag{B.5}$$

where:

N_a = actual particle concentration
W = beam width
v = airspeed
L_D = depth of field
L_1 = section of the annulus sensitive to coincidence events

The probability of a dead time event is just

$$P_D = \frac{\tau}{T}$$

(B.6)

where:

τ, the cumulative electronic dead time during a given sample period ***T***, is found by

$$\tau = n_m(\tau_2 - \tau_1) + n_o(\tau_3 - \tau_1) \quad \text{for } \tau_3 > \tau_1$$

$$\tau = n_m(\tau_2 - \tau_1) \quad \text{for } \tau_3 < \tau_1$$

(B.7)

where:

τ_2 = slow reset delay time

τ_3 = fast reset delay time

n_o = all particles that pass outside the DOF

Then

$$N_m = N_a \frac{(T - \tau)}{T} e^{-\lambda \tau_1}$$

(B.8)

To solve directly for N_a requires an iterative procedure, since N_a is also in the exponential term. The magnitudes of coincidence and dead time losses are shown graphically in Figure B.1, where they are plotted as a percentage of the total number of particles passing through the viewing volume.

FSSP FUNCTION VARIABLES

Several variables are typically output which give a record of the FSSP probe operation. These are used in both sample volume determination and dead time calculations. A few of these variables are listed below.

FSSP Fast Resets (cnts) - FRESET

This variable records the number of fast resets that occur during the FSSP sampling. A fast reset occurs when a particle traverses the beam outside the depth of field. When this occurs, the probe electronics must be reset. This variable is required to account for the probes total dead time. (The fast reset time is determined in the laboratory.)

FSSP Total Strobes (cnts) - FSTROB

This variable records the number of particles which traverse within the depth of field both inside and outside the "effective beam diameter". The "effective beam diameter" is that portion of the beam defined by velocity averaging circuitry contained in the FSSP. That velocity averaging circuitry is designed to reject particles passing through the outer portions

of the beam in order to provide a more accurate sizing (within this "effective beam diameter"). The velocity averaging circuitry keeps track of particle transit times and rejects those which are below a certain, probe dependent threshold.

FSSP Beam Fraction - FBMFR

This is a derived variable that is the ratio of the number of velocity-accepted particles (particles that pass through the effective beam diameter) to the total number of particles detected in the depth-of-field of the beam.

$$FBMFR = FSSP / FSTROB$$

where:

FSSP = the total number of particles velocity-accepted by the FSSP

FSSP-100 Calculated Activity Fraction (none) - FACT

This is the calculated FSSP probe activity. It represents the probe dead time, the time the probe electronics are busy processing particle data. The probe activity is calculated from fast resets, total strobes, and both slow and fast reset times (determined in the laboratory).

$$FACT = (FSTROB)\ \tau_2 + (FRESET)\ \tau_3$$

where:

τ_2 = slow reset time

τ_3 = fast reset time

At the request of the user, 2D data will be processed by the RAF Data Management Group on the CRAY-1 at the Scientific Computing Division. Since the images may be interpreted in a variety of ways, the user will be asked to select from a number of available options before the processing begins.

APPENDIX C.

Liquid Water Content Calculations

PMS/CSIRO Liquid Water Content

The electrical power required to maintain the sensor of this probe at a constant temperature must compensate for heat losses from the sensor to the passing air stream and to that absorbed by impinging droplets. This is expressed through an energy balance equation as:

$$P = P \quad + P$$

$$d \qquad w$$

(C.1)

where the losses to the air, P_d, are described by

$$P_d = \text{pi}\ k\ (T_s - T_a)\ Nu$$

(C.2)

and the losses to the droplets, P_w, are similarly expressed as

$$P_w = l\ d\ w\ v\ [L_v + c\ (T_b - T_a)]$$

(C.3)

where:

pi = 3.14159...
Nu = Nusselt number
k = thermal conductivity of dry air
l = length of sensor
d = diameter of sensor
T_s = temperature of sensor
T_a = temperature of air
T_b = boiling point of water
c = specific heat of water
v = airspeed
w = liquid water content

The liquid water content can be immediately obtained by measuring the power ***P***, if the value for the Nusselt number is known. The Nusselt number can be determined as a function of the Reynolds number, ***Re***, that takes the form of a power law

$$Nu = A\ Re^x$$

(C.4)

where ***A*** and ***x*** are determined empirically from flight data taken at several altitudes and airspeeds.

JW Baseline Drift Removal

The compensation wire in the JW partially removes the effects of convective heat losses from the JW measurements. However, the compensation is affected by changes in temperature and pressure, and oftentimes the zero baseline of the instrument will drift by 0.2 to 0.3 g/M^3 when out of cloud. This zero offset can be removed when the FSSP is present by using this probe to detect the presence of cloud. When the FSSP indicates the absence of cloud, a running average is maintained of the JW-measured LWC. During the cloud penetration, this average offset value is subtracted from the measurement.

Rosemount Ice Detector LWC Calculations

The voltage output of the Rosemount ice detector is directly proportional to the mass of ice that accretes on the sensor. When the aircraft is in cloud, the voltage increases steadily as ice builds on the sensor up to the point that a preset threshold is reached and the sensor heat is activated to remove the ice. An estimate of the LWC can be made from the voltage rate of change if several assumptions are made. The mass accumulated on the sensor is determined by:

$$m = E_c\, d\, l\, v\, w\, t \tag{C.5}$$

where:

E_c = droplet collection efficiency of the sensor
d = diameter of the sensor
l = length of the sensor
v = aircraft velocity
w = liquid water content
t = accumulation time

Thus the mass accumulation rate is:

$$dm/dt = k\, w \tag{C.6}$$

where:

$$k = E_c\, d\, l\, v \tag{C.7}$$

The voltage-to-mass calibration factor is determined either in laboratory calibrations or with in-flight comparisons with other LWC measurements. If the voltage-to-mass calibration is described by:

$$V = G\, m \tag{C.8}$$

then:

$$dV/dt = G\, dm/dt \tag{C.9}$$

and solving for the LWC, w,

$$w = (l\, dV)/(Gk\, t) \tag{C.10}$$

This expression for the LWC can be evaluated if the collection efficiency is known and if the diameter and length of the sensor can be assumed to be constant. These assumptions involve

some uncertainty, since the collection efficiency is a function of the diameter of the sensor, the size of the water droplets, the speed of the aircraft, and the temperature and viscosity of the air. The estimated uncertainty in collection efficiency is on the order of 20%.

An additional uncertainty in the evaluation of Equation C.10 arises because of the assumption of constant diameter and length of the sensor. Wind tunnel and laboratory tests have shown that ice does not accumulate evenly on the ice probe sensor because of aerodynamic effects around the probe. Thus the value of l is variable depending upon the environmental conditions. The ice mass that builds on the sensor changes the effective cross section of the probe, so that the value of ***d*** changes as a function of time, airspeed and liquid water content. There is a 30% uncertainty in estimating the sample volume because of these factors.

Finally, the gain ***G***, is a function of where the ice accretes to the sensor and can change as much as 30% during the accumulation period depending upon the accretion pattern.

The total uncertainty in estimating the LWC from Equation C.10 is approximately 50% if the theoretical derivation of ***w*** is used along with the estimates of collection efficiency, sample volume, and voltage-to-mass calibration. However, the value of the product ***Gk*** can be determined empirically without having to assume specific values for the components that go into the derivation of these variables. If ***Gk*** is determined by comparisons with the LWC from the hot-wire probes, the resulting accuracy in the derived LWC is decreased to approximately 20%.

APPENDIX D.

Spurious Image Rejection Techniques in the Processing of Data from the 2D Probe

The 2D probes capture the image of particles in the shape of shadows that pass across the linear array of diodes. Some of these images are not truly representative of real particles but are the result of splashing or breakup of ice or water on the probe arm tips. In especially heavy concentrations of raindrops, liquid water content, or graupel, the rate at which these spurious images are generated can be high and will seriously bias the derived concentrations and size distributions. The remainder of this appendix describes each type of spurious image, its cause, and the pattern recognition technique used to identify and reject it.

Short Arrival Time Rejection

When a particle strikes the arm tip of the probe, the result is a cloud of secondary particles that stream through the probe's sample volume. (See Figure D.1.) The distance between these particles will be quite small, and the measured particle interarrival times also will be very short. On the average, cloud particles are distributed homogeneously and the spacing between them is random and determined by the average concentration, ***C***. Although some of the distances between particles can be short, on average, the spacing is:

$$I_a = (1/C)^{1/3}$$

(D.1)

Thus, when particles in the size range of the 2D probes are even in modest concentrations of 1 to 10 per liter, the average spacing is on the order of 5 to 10 cM.

A 2D probe measures the distance between particles along with the particle image. The majority of spurious particles generated by collisions with the probe tips will be rejected if a threshold is specified that is much smaller than the average expected spacing between particles. This threshold will eliminate some legitimate particles, of course, since there is a finite probability that the spacing between some particles is very short. The fraction of particles erroneously eliminated can be calculated if the particles are assumed to be distributed randomly in space with an exponential probability distribution function:

$$P(l < l_t) = 1 - e^{-l_t/l_a}$$

(D.2)

where:

l = distance between particles
l_t = threshold distance

Hollow and Gapped Particle Rejection

Another characteristic of particles created spuriously by arm tip collision is that they will be so close together that the probe cannot recognize the end of one particle and the start of another, and the result is an image that looks like a number of distinct particles in the same image frame. This condition is detected in the analysis in two different ways. Sometimes several blank image slices will occur within the image. (See Figure D.2.) When this condition is detected, the particle is rejected. The other method is to measure the ratio of the area of the shadow image to the area of the rectangle that would enclose the image and reject the image if this ratio is less than a preset threshold. This fraction (shown graphically in Figure D.3) is determined by:

$$f = A/(XY)$$

(D.3)

where A is the image area expressed in number of diodes shadowed and X and Y are the lengths of the sides of the rectangle that circumscribe the image. These lengths are also expressed in terms of the number of diodes.

The threshold is usually set to 0.4, a value that has been determined empirically after visually examining a large number of spurious 2D images and calculating the average fraction, f, from Equation D.3.

Water Streamer Rejection

Under conditions of heavy liquid water content, pools of water will build on the splashguards of the probe and eventually be discharged across the opening in the arm tip and will appear as an elongated image. (See Figure D.4.) These images are rejected by comparing the length of the particle along the direction of flight to its width along the diode array. If the length is greater than six times the width, the particle is assumed to be a "streaker" and is rejected. This criterion will

also sometimes reject larger particle or particles only partially in the sample volume. To minimize rejecting too many of these types of particle, extra constraints are imposed on the rejection criterion. When the width of the particle is greater than three-quarters of the array width, or if any of the diode array end elements are shadowed, then the rejection criterion is not imposed.

Blank Image Rejection

The 2D probe will often register the occurrence of a particle, but the resulting image frame will be blank. The "zero area" images are usually the result of particles whose size is of the same order as the resolution of the probe. When a particle enters the beam, the 2D probe is placed in a ready state and waits until the occurrence of the next cycle of the timing clock (which is called the "true air speed clock," since the frequency is proportional to the aircraft velocity). If the particle is small, it will have passed completely across the array by the time the next clock cycle occurs. In these cases, the shadow state of the diodes is not captured in time, yet the event is still recorded by the probe by the appropriate time word in the data buffer.

Most of these zero-area events are caused by legitimate particles and could be used to calculate the total concentration; however, it is left to the discretion of the investigator whether or not to reject these events and exclude them from the analysis of the data.

Bibliography

Baumgardner, D., and J.E. Dye, 1982: Cloud particle measurement symposium: Summaries and Abstracts, ***NCAR Tech. Note NCAR/TN-199+PROC***, 103 pp.

_____ and _____, 1983a: The 1982 cloud particle measurement symposium, ***Bull. Amer. Meteorol. Soc.***, **64**, 336-370.

_____ and _____, 1983b: A discussion of FSSP data reduction techniques, ***Preprints of the 1983 AMS 5th Symposium on Meteorological Observations and Instrumentation***, April 11-15, Toronto, Ontario.

Baumgardner, D., 1983: An analysis and comparison of five water droplet measuring instruments, ***J. Appl. Meteor.***, **22**, 891-910.

Baumgardner, D., J.W. Strapp, and J.E. Dye, 1985: Evaluation of the forward scattering spectrometer probe Part II: Corrections for coincidence and dead-time losses, ***J. Atmos. and Oceanic Tech.***, **2**, 626-632.

Baumgardner, D., 1986: A new technique for the study of cloud microstructure, ***J. Oceanic and Atmos. Tech.***, **3**, 340-343.

Baumgardner, D., J.E. Dye, and W.A. Cooper, 1986: The effects of measurement uncertainties on the analysis of cloud particle data, ***Preprints 23rd Conf. Cloud Physics***, Snowmass, Co., 313-316.

Baumgardner, D., 1987: Corrections for the response times of particle measuring probes,

Preprints 6th Symposium Meteor. Obs. and Instr., New Orleans, 148-151.

Brown, E.N., 1982: Ice detector evaluation for aircraft hazard warning and undercooled water content measurements, ***J. Aircraft***, **19**, 980-983.

Dye, J.E., and D. Baumgarnder, 1983: Laboratory evaluations of six forward scattering and spectrometer probes, ***Preprints of the 1982 AMS Cloud Physics Conference***, November, 1982, Chicago, Illinois, 279-281.

_____ and _____, 1984: Evaluation of the forward scattering spectrometer probe Part I: Electronic and optical studies, ***J. Atmos. Ocean. Tech.***, **1**, 330-344.

Heymsfield, A.J. and J.L. Parrish, 1979: Techniques employed in the processing of particle size spectra and state parameter data obtained with the T-28 aircraft platform, ***NCAR Tech. Note NCAR/TN-137+IA***.

Heymsfield, A.J. and D. Baumgardner, 1985: Summary of a workshop on processing 2D probe data, ***Bull. Amer. Meteor. Soc.***, **66**, 437-440.

King, W.D., D.A. Parkin, and R.J. Handsworth, 1978: A hot-wired liquid water device having fully calculable response characteristics, ***J. Appl. Met.***, **17**, 1809-1813.

King, W.D., J.E. Dye, J.W. Strapp, D. Baumgardner, and D. Huffman, 1985: Icing wind tunnel tests on the CSIRO liquid water probe, ***J. Oceanic and Atmos. Tech.***, **2**, 340-352.

Knollenberg, R.G., 1970: The optical array: An alternative to extinction of scattering for particle size measurements, ***J. Appl Meteor.***, **9**, 86-103.

_____, 1972: Comparative liquid water content measurements of conventional instruments with an optical array spectrometer, ***J. Appl. Meteor.***, **11**, 501-508.

_____, 1975: The response of optical array spectrometers to ice and snow: A study of probe size to crystal mass relationship, ***AFCRL-TR-75-0494***, 70 pp.

_____, 1981: Techniques for probe in-cloud microstructure; Clouds, Their Formation, ***Optical Properties, and Effects***, P.V. Hobbs and A. Deepak, Eds., Academic Press, 495 pp.

Kowles, J. 1973: A discussion of icing-rate measurement and the Rosemount icing-rate system, ***Rosemount Rept. 67312A***, 18pp.

MacPherson, J.I. and D. Baumgardner, 1987: Studies of airflow effects about wing-mounted PMS probes, ***Preprints 6th Symposium Meteor. Obs. and Instr.***, New Orleans, 144-147.

Musil, D., and W.R. Sand, 1974-75: Use of the Rosemount icing-rate probe in thunderstorm penetrations, ***Atmospheric Technology***, No. 6, Winter, 140-142.

Neel, C.B., 1973: Measurement of cloud liquid water content with a heated wire, ***19th International ISA Aerospace Instrumentation Symposium***, May, Las Vegas, Nevada.

Strapp, J.W., and R.S. Schemenauer, 1982: Calibrations of Johnson-Williams liquid water content meters in a high-speed icing tunnel. ***J. Appl. Meteor.***, **21**, 98-108.

Last update: Fri Oct 3 14:28:57 MDT 2003

RAF Bulletin No. 24

TABLE 1

INSTRUMENT	MEASUREMENT RANGE	BIN WIDTH µM	VELOCITY RANGE M/s
FSSP[1, 3]	0.5 µM to 7.5 µM diameter[2] 1.0 µM to 15.0 µM diameter 2.0 µM to 32.0 µM diameter 2.0 µM to 47.0 µM diameter	0.5 µM 1.0 µM 2.0 µM 3.0 µM	10 to 200
ASASP	0.12 to 3.12 µM diameter	0.25 to 0.375 µM, progressively weighted	10 to 200
200X	40 µM to 280 µM diameter	20 µM	10 to 200
260X	40 µM to 620 µM diameter	10 µM	10 to 200
200Y	300 µM to 4500 µM diameter	300 µM	10 to 200
2D-C	25 µM to 800 µM diameter	25 µM	10 to 110
2D-P	200 µM to 6400 µM diameter	200 µM	10 to 220
PSM	Variable	Variable	10 to 200
JW	0.1 to 6.0 g/M^3		50 to 200
PMS/CSIRO	0.0 to 3.0 g/M^3		10 to 200
Ice Detector	0.0 to 0.5 0.13 mM of ice		>= 15

[1] Size ranges programmatically changable during flight.
[2] Nominal values; calibrated values may vary after airspeed corrections.
[3] Size corrections are applied to data for airspeeds > 100 M/s.

Last update: Thu Aug 10 14:27:56 MDT 2000

RAF Bulletin No. 24

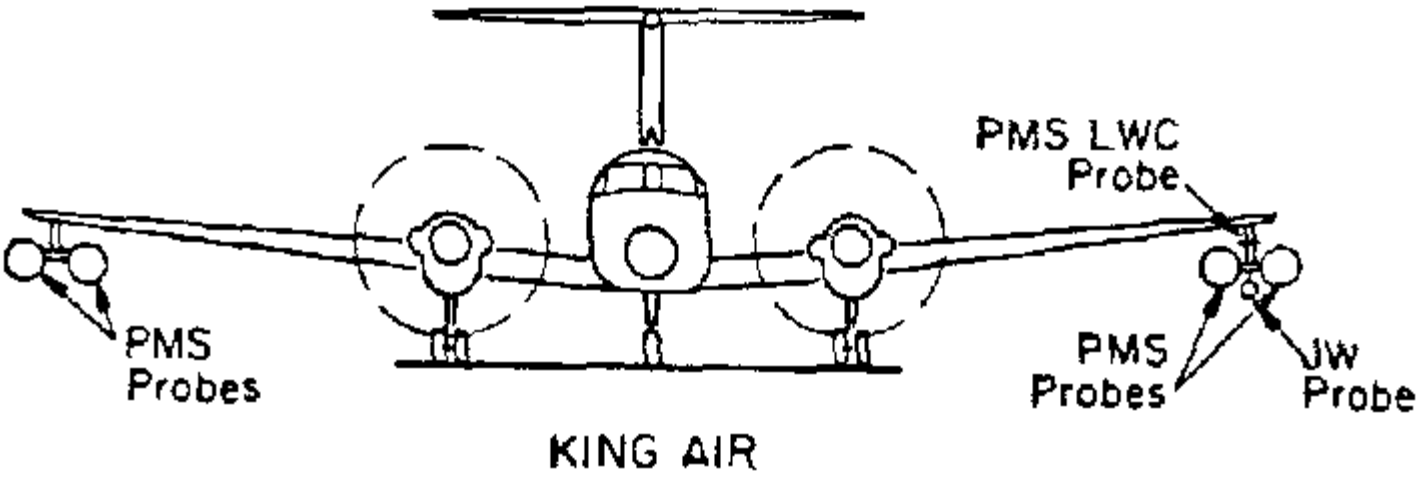

Figure 1. A schematic representation illustrating locations of PMS and hot-wire liquid water content probes on the (former) NCAR King-Air aircraft

---

Last update: Wed Dec 6 13:40:24 MST 2000

Passive Cavity Aerosol Spectrometer Probe

PCASP-100 Aerosol Probe

1. Introduction

The Passive Cavity Aerosol Spectrometer Probe (PCASP) Model 100 is an instrument developed by Particle Measuring Systems (PMS Inc., Boulder, Co) for the measurement of aerosol particle size distributions. This sensor is utilized in studies of tropospheric chemistry and aerosol physics.

2. Operating Principles

The PCASP is of that general class of instruments called optical particle counters (OPCs) that detect single particles and size them by measuring the intensity of light that the particle scatters when passing through a light beam. The schematic diagram shown in Fig. 1 illustrates the optical path of this instrument. A Helium Neon laser beam is focused to a small diameter at the center an aerodynamically focused particle laden air stream. Particles that encounter this beam scatter light in all directions and some of this light is collected by a mangin mirror over angles from about 35^{o} - 135^{o}. This collected light is focussed onto a photodetector and then amplified, conditioned, digitized and classified into one of fifteen size channels. The size of the particle is determined by measuring the light scattering intensity and using Mie scattering theory to relate this intensity to the particle size. Figure 2 illustrates how the scattered light varies with particle diameter given that the particle is spherical and that the refractive index is known. The size information is sent to the data system where the number of particles in each channel is accumulated over a preselected time period. Figure 3 shows a typical size distribution where the concentration of particles in each size category is shown, normalized by the width of the size channel. Figure 4 is a photograph of the PCASP inside a canister that is normally mounted on an aircraft pylon.

3. Sensor Specifications

3a. General Information

Manufacturer: Particle Measuring Systems Inc., Boulder, Co.

RAF Resident Expert: Darrel Baumgardner

(303) 497-1054

darrel@ncar.ucar.edu

Typical Mounting

Location: Pylons on fuselage or wings

Calibration Method: Monodispersed polystyrene latex beads

Range: 0.1 mm - 3.0 mm

Accuracy: ±20% (Diameter)

±16% (Concentration)

3b. Primary Output

RAF Parameter Name Plain Language Name Description

APC01-15 Channels 1-15 15 channels of accumulated counts

3c. Derived Output

RAF Parameter Name Plain Language Name Description

CONCP Concentration # of particles per unit volume - number per cubic centimeter

SFCP Surface Area Total surface area - micrometers squared per cubic centimeter

VOLP Volume Total particle volume - Cubic micrometers per cubic meter

DBARP Average Diameter Arithmetic average of particle size - micrometers

$$CONCP = \sum_{i=1}^{i=15} \frac{n_i}{V} \; ; \; SFCP = \pi \sum_{i=1}^{i=15} \frac{n_i d_i^2}{V} \; ; \; VOLP = \frac{\pi}{6} \sum_{i=1}^{i=15} \frac{n_i d_i^3}{V} \; ; \; DBARP = \frac{\sum_{i=1}^{i=15} n_i d_i}{\sum_{i=1}^{i=15} n_i}$$

1

---

where n_i is the number of particles detected in size channel i, d_i is the diameter represented by channel i, and V is the sample volume measured in a given sample period.

4. Data Interpretation

The PCASP was developed as an aerosol particle measurement instrument. The size that is determined by the PCASP assumes that the scattered light detected is from a spherical particle of refractive index 1.58. The size distributions produced from these measurements must be viewed with great caution when in mixed composition aerosols. Particles will not be correctly sized due to their different refractive index and non-spherical shapes.

The probability of more than a single particle coinciding in the beam or being missed during the electronic reset time increases with concentration. Corrections are applied to account for these losses but still lead to concentration uncertainties.

The PCASP is a particle sizing instrument, not a particle surface area or volume probe. Since the surface areas and volumes are derived by integrating the size distribution, uncertainties in the size measurement lead to root sum squared accuracies in surface area and volume a factor of two and three higher, respectively.

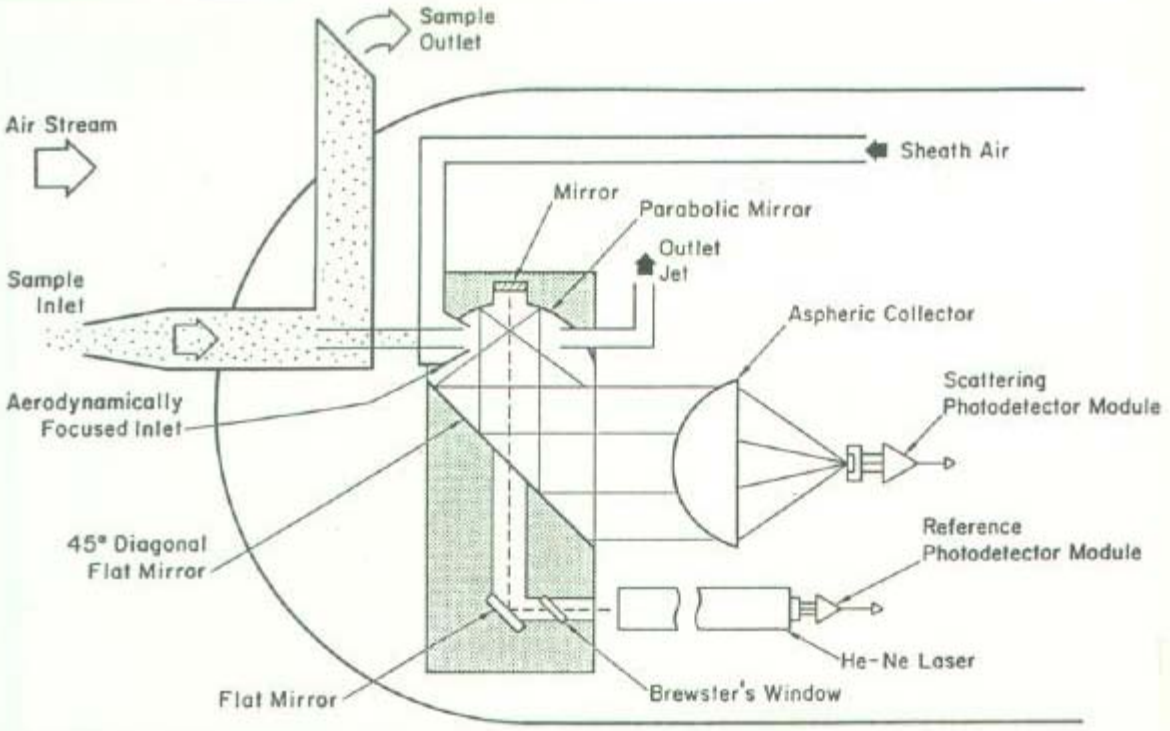

Figure 5.1

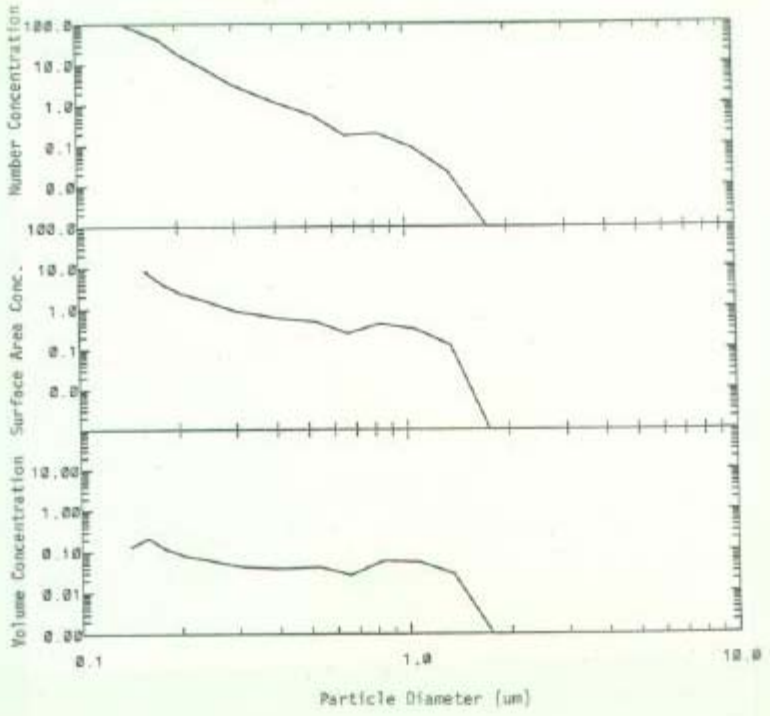

Figure 5.2

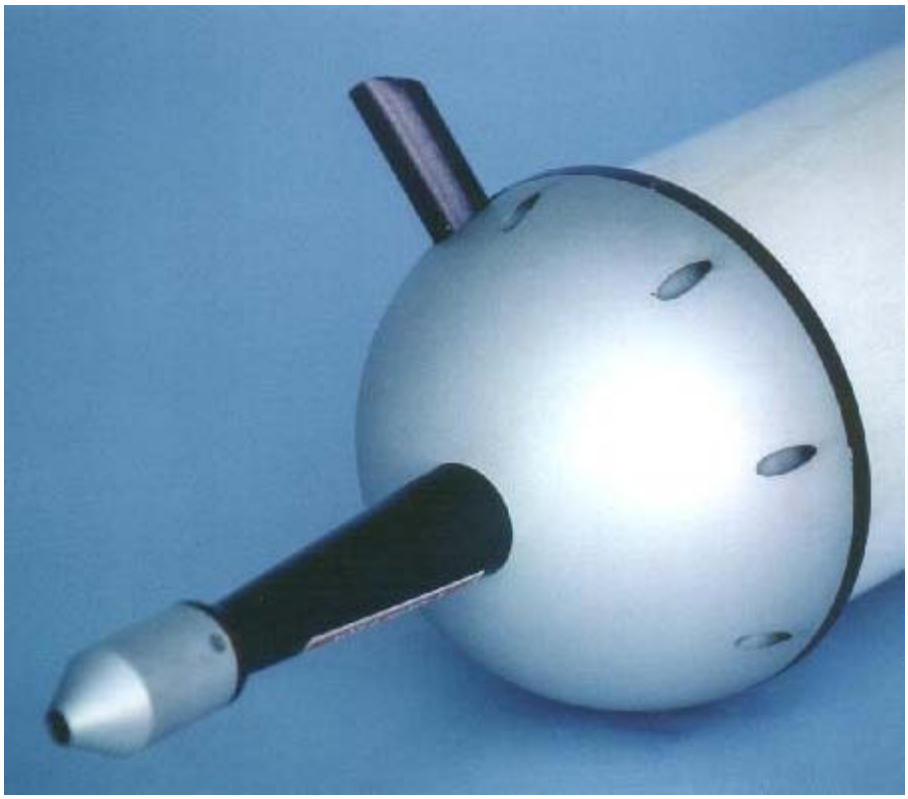

Forward Scattering Spectrometer Probe

FSSP-100 Cloud Probe

1. Introduction

The Forward Scattering Spectrometer Probe (FSSP), model 100, is an instrument developed by Particle Measuring Systems (PMS Inc., Boulder, Co) for the measurement of cloud droplet size distributions. The sensor is used primarily for the study of cloud microphysical processes, particularly the nucleation and growth of cloud droplets through condensation and coalescence.

2. Operating Principles

The FSSP is of that general class of instruments called optical particle counters (OPCs) that detect single particles and size them by measuring the intensity of light that the particle scatters when passing through a light beam. The schematic diagram shown in Fig. 1 illustrates the optical path of this instrument. A Helium Neon laser beam is focused to a diameter of 0.2 mm at the center of an inlet that faces into the oncoming airstream. This laser beam is blocked on the opposite side of the inlet with an optical stop, a "dump spot" to prevent the beam from entering the collection optics. Particles that encounter this beam scatter light in all directions and some of that scattered in the forward direction is directed by a right angle prism though a condensing lens and onto a beam splitter. The "dump spot" on the prism and aperture of the condensing lens define a collection angle from about 4^o - 12^o.

The beam splitter divides the scattered light into two components, each of which impinge on a photodetector. One of these detectors, however, is optically masked to receive only scattered light when the particles pass through the laser beam displaced greater than approximately 1.5 mm either side of the center of focus. Particles that fall in that region are rejected when the signal from the masked detector exceeds that from the unmasked detector. This defines the sample volume needed to calculate particle concentrations.

The size of the particle is determined by measuring the light scattering intensity and using Mie scattering theory to relate this intensity to the particle size. Figure 2 illustrates how the scattered light varies with particle diameter given that the particle is spherical and that the refractive index is known.

The size is categorized into one of 15 channels and this information sent to the data system where the number of particles in each channel is accumulated over a preselected time period. Figure 3 shows a typical size distribution where the concentration of droplets in each size category is shown, normalized by the width of the size channel. Figure 4 is a photograph of the FSSP in the canister that is normally mounted on an aircraft pylon.

3. Sensor Specifications

3a. General Information

Manufacturer: Particle Measuring Systems Inc., Boulder, Co.

RAF Resident Expert: Darrel Baumgardner

(303) 497-1054

darrel@ncar.ucar.edu

Typical Mounting

Location: Pylons on fuselage or wings

Calibration Method: Monodispersed glass beads

Range: 2.0 mm - 47.0 mm

Accuracy: ±20% (Diameter)

±16% (Concentration)

3b. Primary Output

RAF Parameter Name Plain Language Name Description

AFS01-15 Channels 1-15 - 15 channels of accumulated counts

FSTRB Total Strobes Total Particles in depth of field

FRST Fast Resets Total Particles outside depth of field

FACT Activity Fraction of sample period that probe was active

3c. Derived Output

RAF Parameter Name Plain Language Name Description

CONCF Concentration # of droplets per unit volume - number per cubic centimeter

PLWCF Liquid Water Content Total droplet mass -

grams per cubic meter

DBARF Average Diameter Arithmetic average of droplet size - micrometers

$$CONCF = \sum_{i=1}^{i=15} \frac{n_i}{V} \; ; \; PLWCF = \frac{\pi}{6} \rho \sum_{i=1}^{i=15} \frac{n_i d_i^3}{V} \; ; \_ DBARF = \frac{\sum_{i=1}^{i=15} n_i d_i}{\sum_{i=1}^{i=15} n_i}$$

1

---

where n_i is the number of droplets detected in size channel i, d_i is the diameter represented by channel i, and V is the sample volume measured in a given sample period.

4. Data Interpretation

The FSSP-100 was developed as a cloud droplet measurement instrument. The size that is determined by the FSSP assumes that the scattered light detected is from a spherical, liquid droplet of refractive index 1.33. The size distributions produced from these measurements must be viewed with great caution when in clouds containing mixtures of water and ice, since ice particles will not be correctly sized due to their different refractive index and non-spherical shapes.

A secondary caution is when looking at size distributions when precipitation sized drops are presents. These are suspected of colliding with the sample inlet and causing spurious satellite droplets.

The probability of more than a single particle coinciding in the beam or being missed during the electronic reset time increases with concentration from about 5% losses at 300

cm^{-3} to greater than 30% at 1000 cm^{-3}. Corrections are applied to account for these losses but still lead to concentration uncertainties.

The FSSP is a droplet sizing instrument, not a liquid water content probe. Since the liquid water content is derived by integrating the size distribution, uncertainties in the size measurement lead to root sum squared accuracies in liquid water content a factor of three higher.

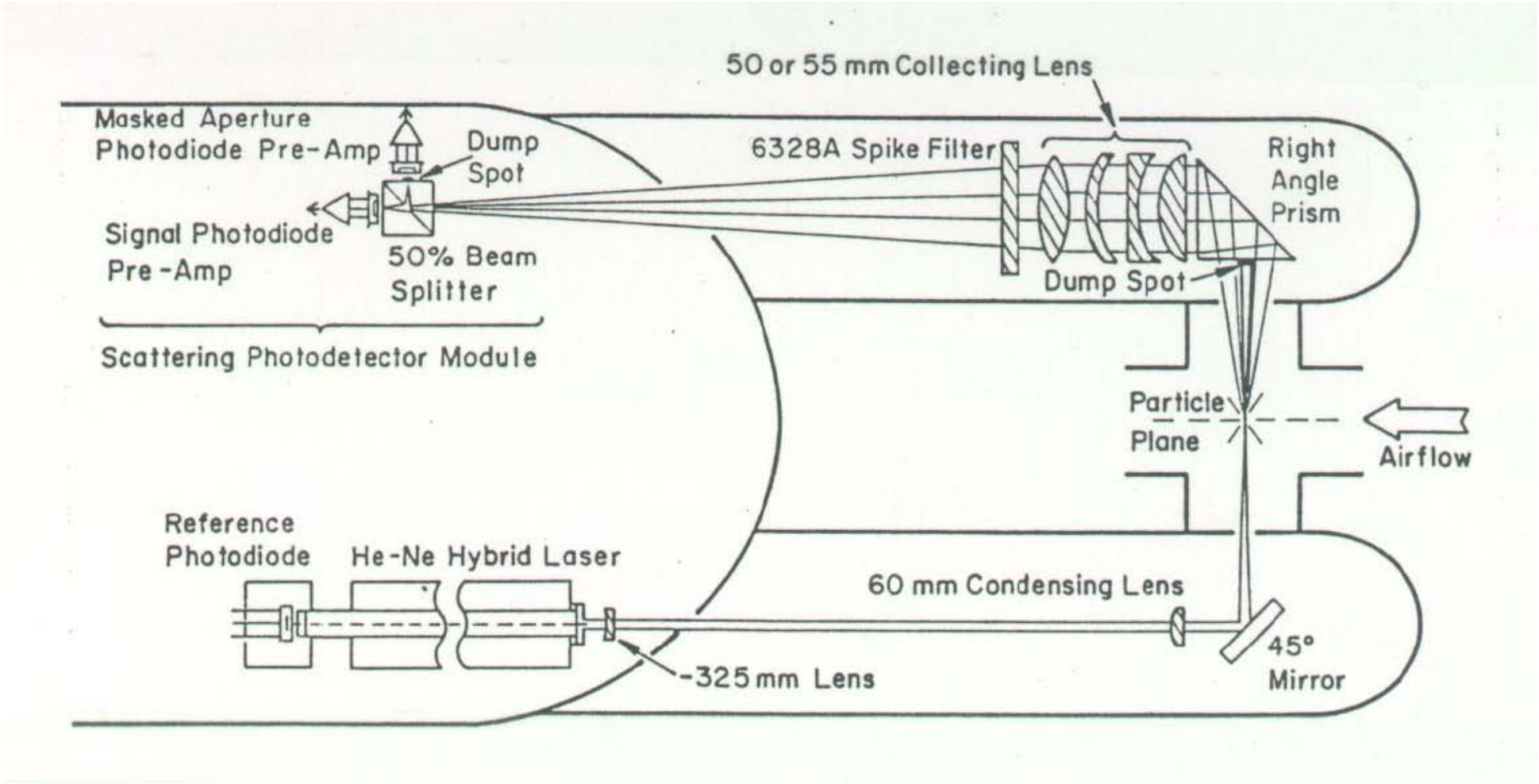

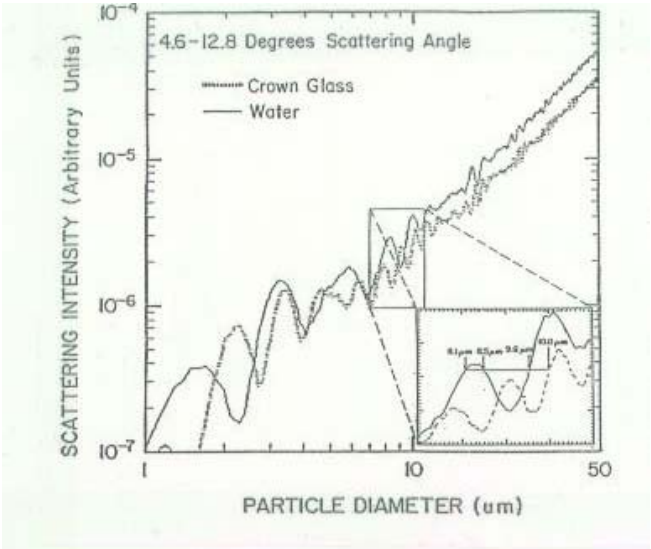
4.6-12.8 Degrees Scattering Angle
Crown Glass
Water
SCATTERING INTENSITY (Arbitrary Units)
PARTICLE DIAMETER (um)
1
10
50

Figure 5.5

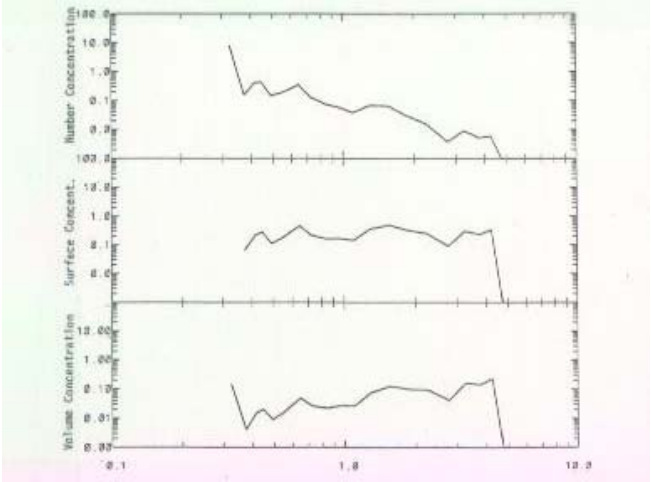
Number Concentration
Surface Concent.
Volume Concentration

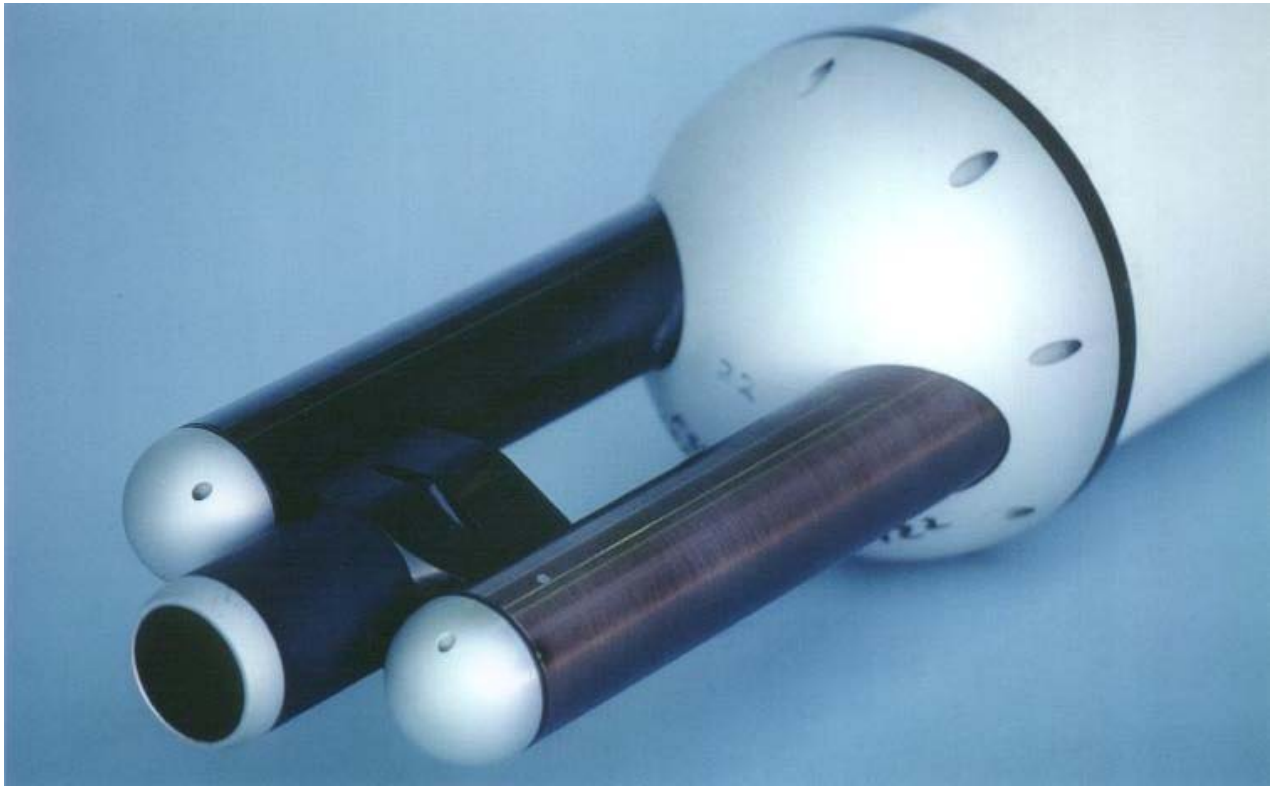

Forward Scattering Spectrometer Probe

FSSP-300 Aerosol Probe

1. Introduction

The Forward Scattering Spectrometer Probe (FSSP) Model 300 is an instrument developed by Particle Measuring Systems (PMS Inc., Boulder, Co) for the measurement of aerosol particle size distributions. The sensor was originally developed for the study of stratospheric aerosol distributions and polar stratospheric clouds but is now widely utilized in studies of tropospheric chemistry and aerosol physics.

2. Operating Principles

The FSSP-300 is of that general class of instruments called optical particle counters (OPCs) that detect single particles and size them by measuring the intensity of light that the particle scatters when passing through a light beam. The schematic diagram shown in Fig. 1 illustrates the optical path of this instrument. A Helium Neon laser beam is focused to a small diameter at the center of an inlet that faces into the oncoming airstream. This laser beam is blocked on the opposite side of the inlet with an optical stop, a "dump spot" to prevent the beam from entering the collection optics. Particles that encounter this beam scatter light in all directions and some of that scattered in the forward direction is directed by a right angle prism though a condensing lens and onto a beam splitter. The "dump spot" on the prism and aperture of the condensing lens define a collection angle from about 4^o - 12^o.

The beam splitter divides the scattered light into two components, each of which impinge on a photodetector. One of these detectors, however, is optically masked to receive only scattered light when the particles pass through the laser beam within a region 0.5 mm either side of the center of focus. Particles that fall outside that region are rejected when the signal from the unmasked detector exceeds that from the masked detector. This defines the sample volume that is needed in order to calculate particle concentrations.

The size of the particle is determined by measuring the light scattering intensity and using Mie scattering theory to relate this intensity to the particle size. Figure 2 illustrates how the scattered light varies with particle diameter given that the particle is spherical and that the refractive index is known. The size is categorized into one of 31 channels and this information is sent to the data system where the number of particles in each channel is accumulated over a preselected time period. Figure 3 shows a typical size distribution where the concentration of particles in each size category is shown, normalized by the width of the size channel. Figure 4 is a photograph of the FSSP-300 in the canister that is normally mounted on an aircraft pylon.

3. Sensor Specifications

3a. General Information

Manufacturer: Particle Measuring Systems Inc., Boulder, Co.

RAF Resident Expert: Darrel Baumgardner

(303) 497-1054

darrel@ncar.ucar.edu

Typical Mounting

Location: Pylons on fuselage or wings

Calibration Method: Monodispersed polystyrene latex beads

Range: 0.3 mm - 20.0 mm

Accuracy: ±20% (Diameter)

±16% (Concentration)

3b. Primary Output

RAF Parameter Name Plain Language Name Description

AF301-15 Channels 1-31 31 channels of accumulated counts

FRST3 Total Resets Total Particles passing through the beam

3c. Derived Output

RAF Parameter Name Plain Language Name Description

CONC3 Concentration # of particles per unit volume - number per cubic centimeter

SFC3 Surface Area Total surface area - micrometers squared per cubic centimeter

VOL3 Volume Total particle volume -

Cubic micrometers per cubic meter

DBAR3 Average Diameter Arithmetic average of particle size - micrometers

$$CONC3 = \sum_{i=1}^{i=15} \frac{n_i}{V} \; ; \; SFC3 = \pi \sum_{i=1}^{i=15} \frac{n_i d_i^2}{V} \; ; \; VOL3 = \frac{\pi}{6} \sum_{i=1}^{i=15} \frac{n_i d_i^3}{V} \; ; \; DBAR3 = \frac{\sum_{i=1}^{i=15} n_i d_i}{\sum_{i=1}^{i=15} n_i}$$

(1)

where n_i is the number of particles detected in size channel i, d_i is the diameter represented by channel i, and V is the sample volume measured in a given sample period.

4. Data Interpretation

The FSSP-300 was developed as an aerosol particle measurement instrument. The size that is determined by the FSSP assumes that the scattered light detected is from a spherical particle of refractive index 1.58. The size distributions produced from these measurements must be viewed with great caution when in mixed composition aerosols. Particles will not be correctly sized due to their different refractive index and non-spherical shapes.

The probability of more than a single particle coinciding in the beam or being missed during the electronic reset time increases with concentration from about 5% losses at 300 cm^{-3} to greater than 30% at 1000 cm^{-3}. Corrections are applied to account for these losses but still lead to concentration uncertainties.

The FSSP is a particle sizing instrument, not a particle surface area or volume probe. Since the surface areas and volumes are derived by integrating the size distribution, uncertainties in the size measurement lead to root sum squared accuracies in surface area and volume a factor of two and three higher, respectively.

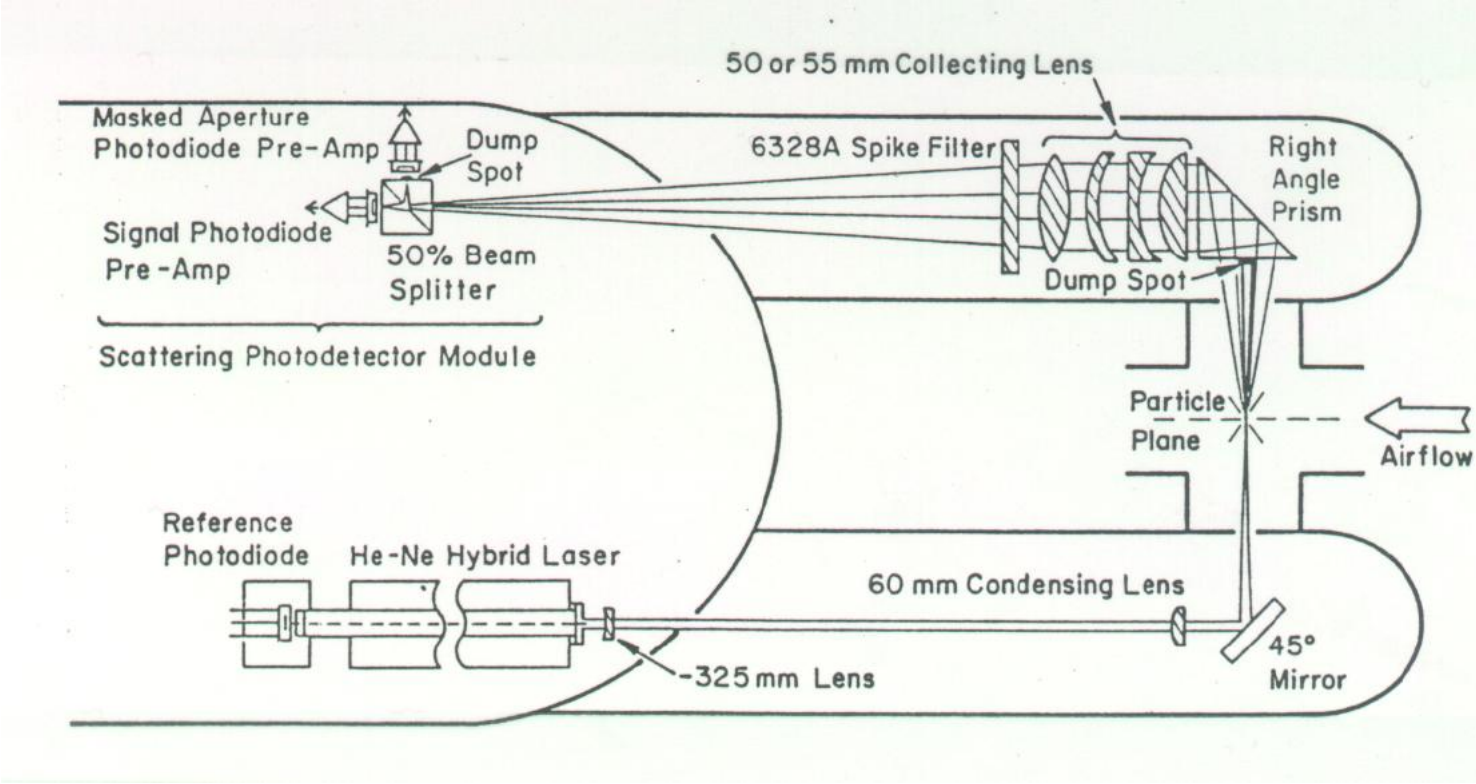

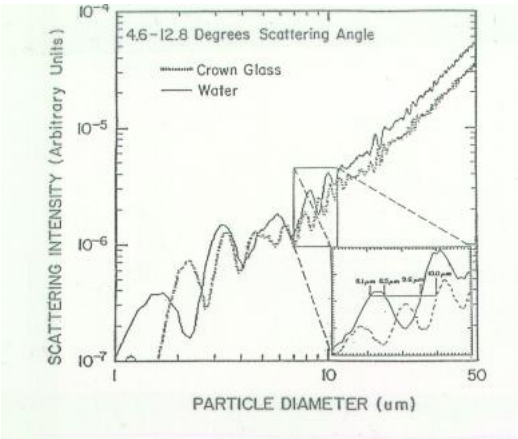
4.6 - 12.8 Degrees Scattering Angle
Crown Glass
Water
SCATTERING INTENSITY (Arbitrary Units)
PARTICLE DIAMETER (um)

Figure 5.5

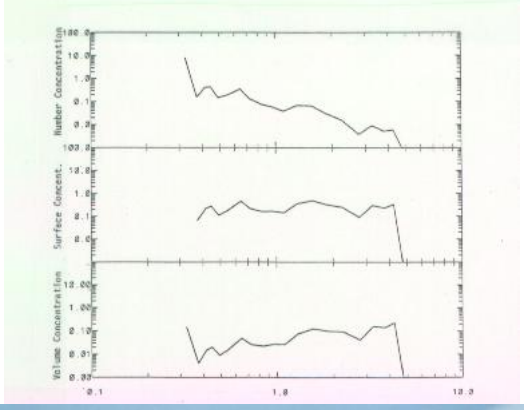
Number Concentration
Surface Concent.
Volume Concentration

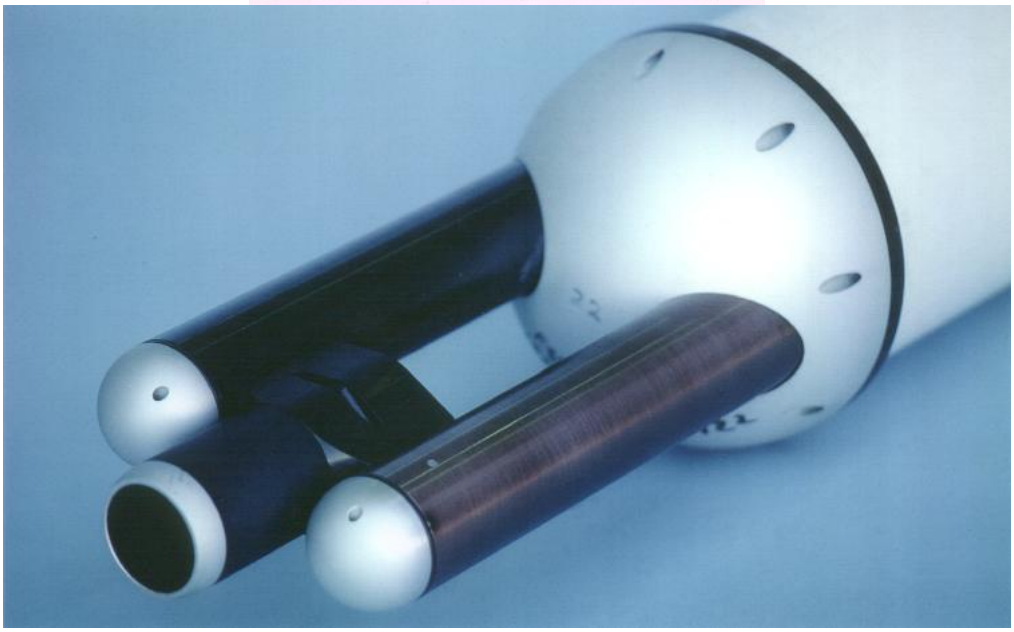

One Dimensional Optical Array Probe

260X OAP Cloud Probe

1. Introduction

The One dimensional optical array probe (1D-OAP), model 260X, is an instrument developed by Particle Measuring Systems (PMS Inc., Boulder, Co) for the measurement of cloud droplet size distributions. The sensor is used primarily for the study of cloud microphysical processes, particularly the growth of cloud droplets through condensation and coalescence into drizzle and precipitation drops.

2. Operating Principles

The 260X measures the size of hydrometeors from the maximum width of their shadow as they pass through a focussed He-Ne laser beam (Fig. 1). The shadow is cast onto a linear diode array and the total number of occulted diodes during the particle's passage represents its size. The diodes at each end of the array act as a mechanism for rejecting those particles that would be undersized when they do not pass entirely within the bounds of the array.

The size is categorized into one of 60 channels and this information is sent to the data system where the number of particles in each channel is accumulated over a preselected time period. Figure 2 shows a typical size distribution where the concentration of droplets in each size category is shown, normalized by the width of the size channel. Figure 3 is a photograph of the 260X in the canister that is normally mounted on an aircraft pylon.

3. Sensor Specifications

3a. General Information

Manufacturer: Particle Measuring Systems Inc., Boulder, Co.

RAF Resident Expert: Darrel Baumgardner

(303) 497-1054

darrel@ncar.ucar.edu

Typical Mounting

Location: Pylons on fuselage or wings

Calibration Method: Monodispersed glass beads

Range: 40 mm - 600 mm

Accuracy: Diameter: Function of particle size, shape and orientation

Concentration: Function of particle size

3b. Primary Output

RAF Parameter Name Plain Language Name Description

AC601-15 Channels 1-60 - 60 channels of accumulated counts

3c. Derived Output

RAF Parameter Name Plain Language Name Description

CONC6 Concentration # of particles per unit volume - number per cubic centimeter

PLWC6 Liquid Water Content Total droplet mass (assuming spherical water drops) - grams per cubic meter

DBAR6 Average Diameter Arithmetic average of droplet size - micrometers

$$CONCF = \sum_{i=1}^{i=15} \frac{n_i}{V} \; ; \; PLWCF = \frac{\pi}{6} \rho \sum_{i=1}^{i=15} \frac{n_i d_i^3}{V} \; ; \_ \; DBARF = \frac{\sum_{i=1}^{i=15} n_i d_i}{\sum_{i=1}^{i=15} n_i}$$

1

---

where n_i is the number of droplets detected in size channel i, d_i is the diameter represented by channel i, and V is the sample volume measured in a given sample period.

4. Data Interpretation

The electronic response time of the 260X imposes some limitations on the minimum detectable size. A photodiode is registered as shadowed when its output is sensed as changing by at least 50% and at least one diode must change by 67%. The edges of particles will oftentimes be missed and particles in the lower end of the size range can pass undetected when the velocity of a particle through the beam exceeds the response of the probe. At 100 ms^{-1} this imposes a lower size threshold of 30-40mm on the 260X.

The 260X is a particle sizing instrument, not a liquid water content probe. The 260X detects any particles that cause the diode array to be occulted, however, these probes cannot differentiate shapes or particle orientation. If liquid water content information is desired, some fairly loose assumptions must be made with regard to the phase, habit, and density of the particles. These assumptions may lead to significant errors in derived liquid water content.

The sample volume of this instrument is relatively small, and varies with particle size. This imposes a limitation on the minimum sampling time if a statistically significant measurement is to be made.

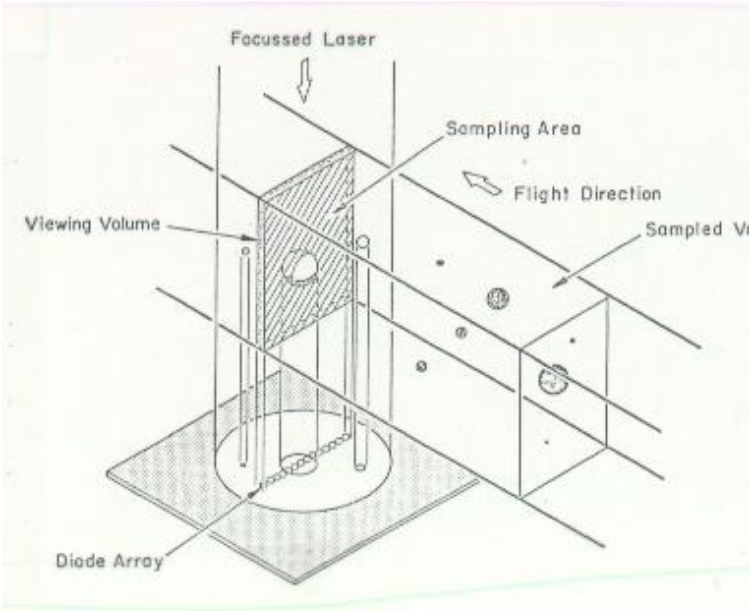
Focussed Laser
Sampling Area
Flight Direction
Viewing Volume
Sampled V
Diode Array

Figure 6.4

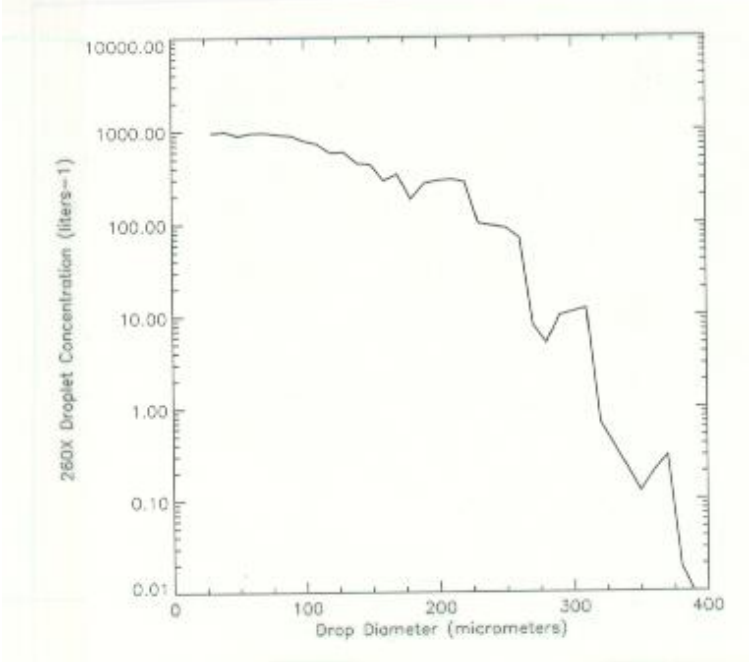
10000.00
1000.00
100.00
10.00
1.00
0.10
0.01
260X Droplet Concentration (liters-1)
0
100
200
300
400
Drop Diameter (micrometers)

Two Dimensional Optical Array Probes

2D Cloud and Precipitation Probes

1. Introduction

The Two dimensional optical array probes (2D-OAP), models 2D-C and 2D-P, are instruments developed by Particle Measuring Systems (PMS Inc., Boulder, Co) for the measurement of cloud and precipitation drop size distributions. These sensors are used primarily for the study of cloud microphysical processes, particularly the growth of cloud drops and ice crystals through aggregation, riming and coalescence into drizzle, rain drops, graupel or other forms of precipitation.

2. Operating Principles

The 2Ds record the two dimensional shadows of hydrometeors as they pass through a focussed He-Ne laser beam (Fig. 1). The shadow is cast onto a linear diode array and the on/off state of these diodes is stored during the particle's passage through the laser beam. This informatio, along with the time that has passed since the previous particle, is sent to the data system and recorded for post-flight analysis.

Information about a particle's shape and size is deduced from analysis of the recorded shadow with a variety of pattern recognition algorithms. Figure 2 illustrates some measurements by the 2D probe in several different types of clouds, ranging from rain drops to pristine ice crystals to more complex heavily rimed ice particles. Figure 3 is a photograph of the 2D-C in the canister that is normally mounted on an aircraft pylon. A complement of 2Ds is normally flown during a project to cover the size range of interest. The 2D cloud probe (2D-C) measures in the range from 25 mm to 800 mm and the 2D precipitation probe (2D-P) measures in the large size range from 200 mm to 6400 mm.

3. Sensor Specifications

3a. General Information

Manufacturer: Particle Measuring Systems Inc., Boulder, Co.

RAF Resident Expert: Darrel Baumgardner

(303) 497-1054

darrel@ncar.ucar.edu

Typical Mounting

Location: Pylons on fuselage or wings

Calibration Method: Monodispersed glass beads and spinning disk with etched dots

Range: 25 mm - 800 mm (2D-C)

200 mm - 6400 mm (2D-P)

Accuracy: Diameter: Function of particle size, shape and orientation

Concentration: Function of particle size

3b. Primary Output

RAF Parameter Name Plain Language Name Description

SDWC1 2D-C Shadow Or Total count of all particles passing through the laser beam of the 2D-C

SDWP1 2D-P Shadow Or Total count of all particles passing through the laser beam of the 2D-P

The raw shadow information is maintained in a compressed format and is left to the user to analyze at their own discretion. Software is available from the RAF to assist in this processing but is not a routine option.

3c. Derived Output

RAF Parameter Name Plain Language Name Description

CON2C? Concentration # of particles per unit volume from the 2D-C probe - number per liter

CON2P? Concentration # of particles per unit volume from the 2D-P probe - number per liter

$$CON2C = SDWC\frac{1}{V_c}\ ;\ CON2P = SDWP\frac{1}{V_p}\ ;\ V_c = DOF \bullet A \bullet v \bullet t\ ;\ DOF = 9482r^2\ ;\ A = W + 4r$$

1

---

where r is the particle radius, W is the diode array width (800 mm and 6400 mm for the 2D-C and 2D-P, respectively), v is the particle velocity and t is the sample period.

4. Data Interpretation

The electronic response time of the 2Ds impose some limitations on the minimum detectable size. A photodiode is registered as shadowed when its output is sensed as changing by at least 50%. The edges of particles will oftentimes be missed and particles in the lower end of the size range can pass undetected when the velocity of a particle through the beam exceeds the response of the probe. At 100 ms^{-1} this imposes a lower size threshold of 30-40mm on the 2D.

The 2Ds are particle imaging instruments, not liquid water content probes. The 2Ds are able to capture a lot of information about a particle just from its shadow, however, if the water content of ice particles is desired, some fairly loose assumptions must be made with regard to the phase, habit, and density of the particles. These assumptions may lead to significant errors in derived liquid water content. A number of pattern recognition algorithms have been developed for analyzing 2D data; however, none of them work very efficiently for any but the most simple of partice shapes.

The sample volume of these instrument is relatively small with respect to the normally low concentrations typically encountered in clouds. This imposes a limitation on the minimum sampling time if a statistically significant measurement is to be made.

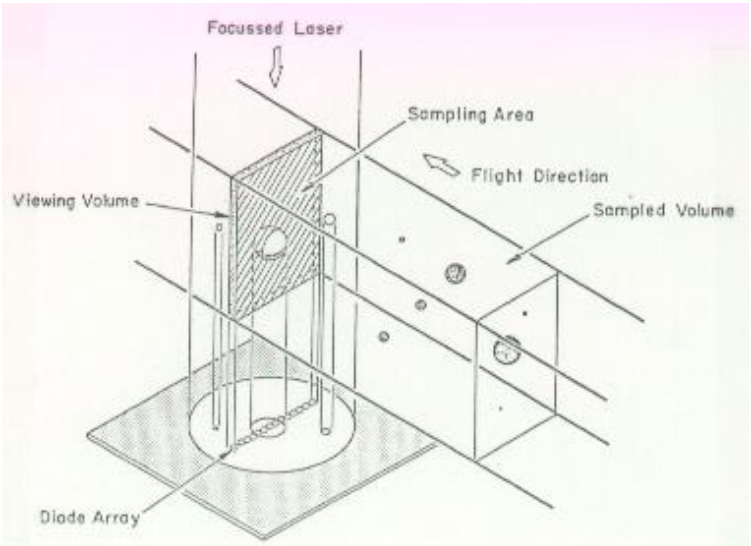
Focussed Laser
Sampling Area
Flight Direction
Viewing Volume
Sampled Volume
Diode Array

Figure 6.7

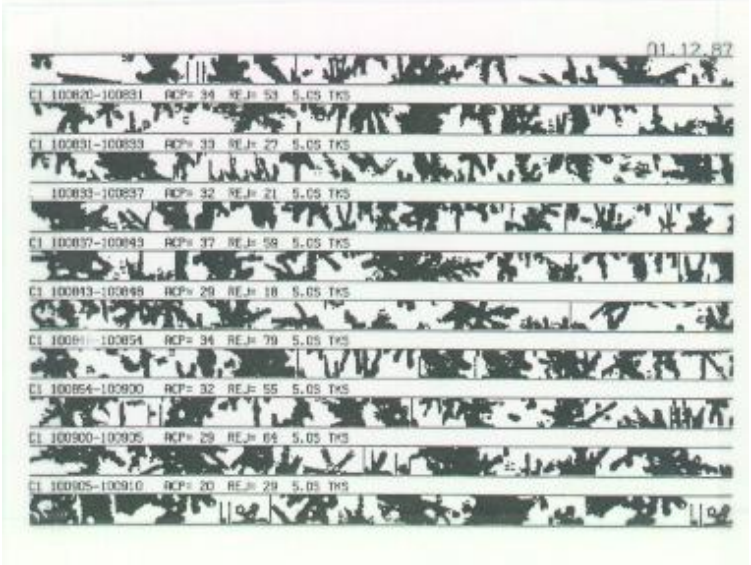
01.12.87
C1 100820-100831 ACP= 34 REJ= 53 5.05 TAS
C1 100831-100833 ACP= 33 REJ= 27 5.05 TAS
100833-100837 ACP= 32 REJ= 21 5.05 TAS
C1 100837-100843 ACP= 37 REJ= 58 5.05 TAS
C1 100843-100848 ACP= 29 REJ= 18 5.05 TAS
C1 100851-100854 ACP= 34 REJ= 79 5.05 TAS
C1 100854-100900 ACP= 32 REJ= 55 5.05 TAS
C1 100900-100905 ACP= 29 REJ= 64 5.05 TAS
C1 100905-100910 ACP= 20 REJ= 29 5.05 TAS

PMS/CSIRO Hot Wire Liquid Water Probe

1. Introduction

The PMS/CSIRO is an instrument developed by Warren King (CSIRO) and marketed by Particle Measuring Systems (PMS Inc., Boulder, Co) for the measurement of cloud liquid water content. This sensor, commonly referred to as the "King" probe, is used primarily for the study of cloud microphysical processes and in icing studies.

2. Operating Principles

The King probe operates under the principle that liquid water can be calculated from measurements of the amount of heat released when vaporized. As shown in the drawing in Fig. 1 and photograph in Fig 2, a heated cylinder is exposed to the airstream and intercepts on coming droplets. The electronics maintain this sensor at a constant temperature (approximately 130^{o} C) and monitor the power required to regulate the temperature as droplets vaporize. This power is directly related to the amount of heat taken away by convection plus the heat of vaporization. The convective heat losses are known empirically and vary with airspeed, temperature and pressure. The liquid water content is calculated from power loss found from the difference between total and convective power losses.

3. Sensor Specifications

3a. General Information

Manufacturer: Particle Measuring Systems Inc., Boulder, Co.

RAF Resident Expert: Darrel Baumgardner

(303) 497-1054

darrel@ncar.ucar.edu

Typical Mounting

Location: Pylons on fuselage or wings

Calibration Method: None required

Range: .05 - 3.0 g m^{-3}

Accuracy: ±15%

3b. Primary Output

RAF Parameter Name Plain Language Name Description

PLWC Power This is the power consumed in watts to maintain the hot wire sensor at a constant temperature.

3c. Derived Output

RAF Parameter Name Plain Language Name Description

PLWCC Liquid Water Content Cloud Droplet water mass - grams per cubic meter

$$PLWCC = \frac{P - P_d}{ldv[L_v + c(T_b - T_a)]} \; ; \; P_d = A_0 \pi k (T_s - T_a) Re^x Pr^y$$

1

---

where l is the sensor length, d is its width, v is the air velocity, L_v is the latent heat of vaporization, c is the specific heat of water, T_b is the boiling point of water, T_a is the air temperature, T_s is the sensor temperature, k is the thermal conductivity of the air, Re is the Reynol's number, Pr is the Prandtl number and A_0, x and y are constants for a heated cylinder at high Reynold's number.

4. Data Interpretation

The King probe sensor is limited by collection efficiency considerations on the small droplet end of the spectrum and by vaporization time on the large end. The sensor has a diameter of approximately 2 mm and small water droplets, less than 10 mm will not impact with 100% efficiency as they follow the airflow around the sensor. These losses are typically about 5% for 10 mm droplets but increase to greater than 20% for diameters less than 5 mm. This is normally not a major problem since the largest fraction of the water mass is typically carried in droplets greater than 10 mm. In developing clouds, however, near cloud base where droplets are still quite small, or in cloud edges where entrainment and evaporation is occurring, the underestimation of liquid water content can be significant.

On the large droplet side, the King probe begins to underestimate the liquid water contained in drops larger than 30-40 mm as a result of incomplete evaporation as these larger droplets impact and are carried away by the airstream before sufficient heat has been transferred to vaporize them.

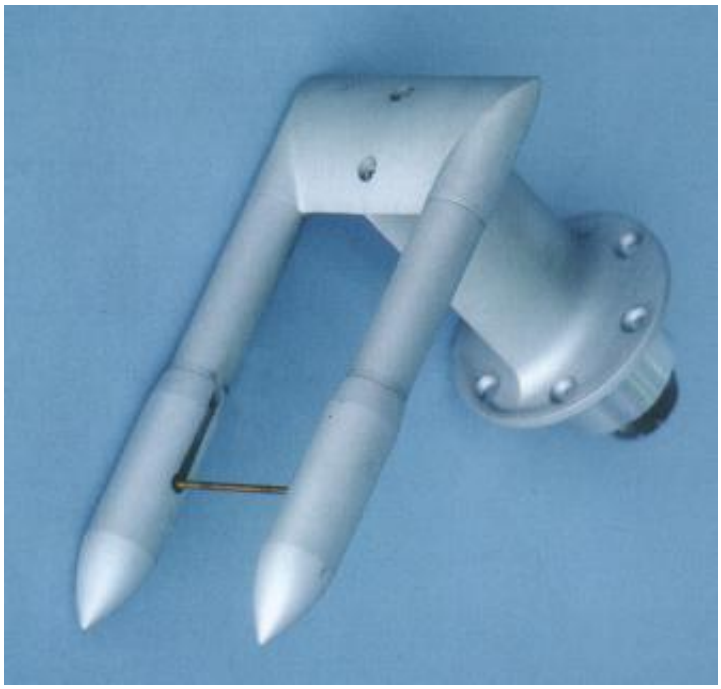

Rosemount Icing Detector

Model 871

1. Introduction

The Model 871 icing detector is an instrument that was developed by Rosemount Engineering (??, Minnesota) for the detection of supercooled liquid water content and the onset of airframe icing. It has been used by the cloud physics community to detect the presence of supercooled water in mixed phase clouds. It has been particularly useful for detecting supercooled water in cirrus clouds at very cold temperatures when the water levels are below the detection limit of conventional hot wire devices.

2. Operating Principles

The Model 871 detector, shown schematically in Fig. 1, measures the amount of ice mass accumulation on a metal cylinder. Using a property known as magnetostriction, the sensing cylinder is driven at a natural frequency of 40 KHz. As the ice accretes on the cylinder, the frequency of the vibration decreases. A phase-locked loop converts this frequency change to a proportional voltage from which the ice mass may be calculated. Once a pre-set amount of mass has been accumulated, the cylinder is heated to melt the ice. Figure 3 shows a typical time history of the probe output as the voltage increases with accumulating ice mass then dropping to its threshold value as the heater is activated to remove the ice.

3. Sensor Specifications

3a. General Information

Manufacturer: Rosemount Engineering, ??

RAF Resident Expert: Darrel Baumgardner

(303) 497-1054

darrel@ncar.ucar.edu

Typical Mounting

Location: Underside of leading edge of the wing

Calibration Method: Single Drop Freezing

Range: .001 - 1.0 g m^{-3} (airspeed and temperature dependent

Accuracy: ±20% - 50%

3b. Primary Output

RAF Parameter Name Plain Language Name Description

?? Detector Volts Out Raw output voltage

3c. Derived Output

RAF Parameter Name Plain Language Name Description

? Liquid Water Content Supercooled liquid water content - grams per cubic meter

$$LWC = \frac{dM}{dt}\frac{1}{E_c dlv} \; ; \; \frac{dM}{dt} = G\frac{dV}{dt}$$

1

---

where l is the sensor length, d is its width, v is the air velocity, E_c is the collection efficiency, and G is the sensitivity coefficient that relates the rate of mass change to voltage change from the sensor.

4. Data Interpretation

The ice detector is limited by collection efficiency considerations on the small droplet end of the spectrum. As ice accumulates and the diameter of the cylinder changes, the collection efficiency decreases. The collection efficiencies are not well characterized but can exceed 20% for droplets less than 10 mm. An additional uncertainty arises due to the change of diameter with mass accumulation. The mass does not accumulate evenly so there is not a simple expression relating the mass to diameter change. A maximum error of 30% is associated with this source of uncertainty.

The sensitivity factor is a function of where the mass accretes on the sensor. This factor can be determined empirically through comparisons with other instruments and can vary depending upon mounting location.

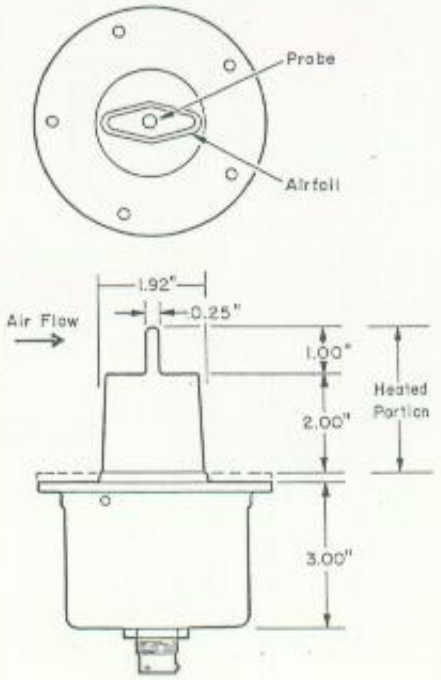
Probe
Airfoil
1.92"
0.25"
Air Flow
1.00"
2.00"
Heated Portion
3.00"

Figure 6.14

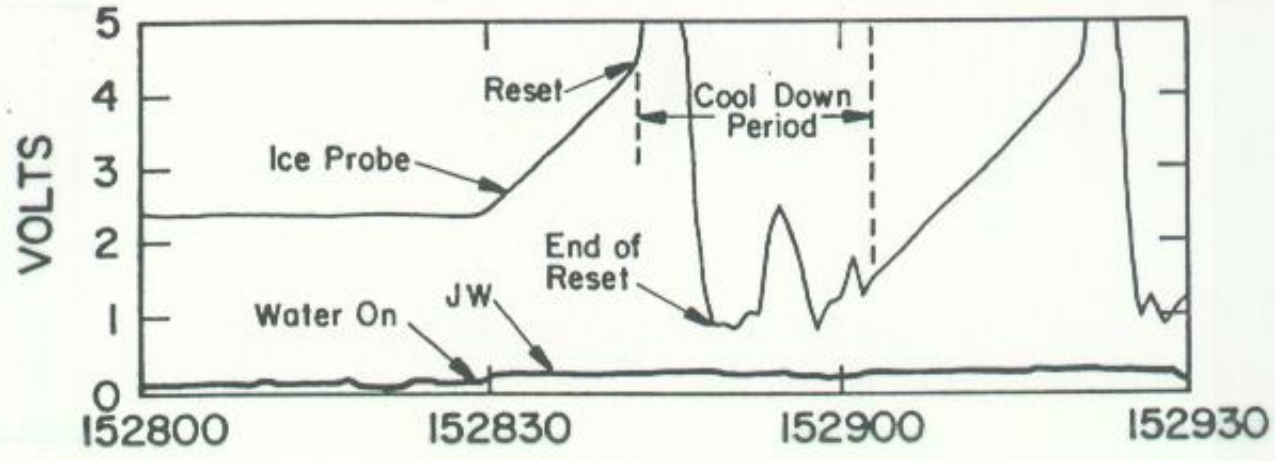
VOLTS
5
4
3
2
1
0
Reset
Cool Down Period
Ice Probe
End of Reset
JW
Water On
152800
152830
152900
152930

Instrument Description

Processing Description and Software

Data Acquisition Software

Data Formats

Data Catalog

Display/Analysis Software

Data Distribution

Summary Datasets

Return to Instrument List

PMS-2D Description

Sample 2-dimensional silhouette of water and ice particles. There are 3 types of 2D probes:

- 2D-C, cloud probe (100 μm to 800 μm with 25 μm resolution).
- 2D-P, precip probe (200 μm to 6.4 mm with 200 μm resolution).
- Greyscale (which produces 64 bit image slice instead of 32).

Picture of a 2D-C probe.

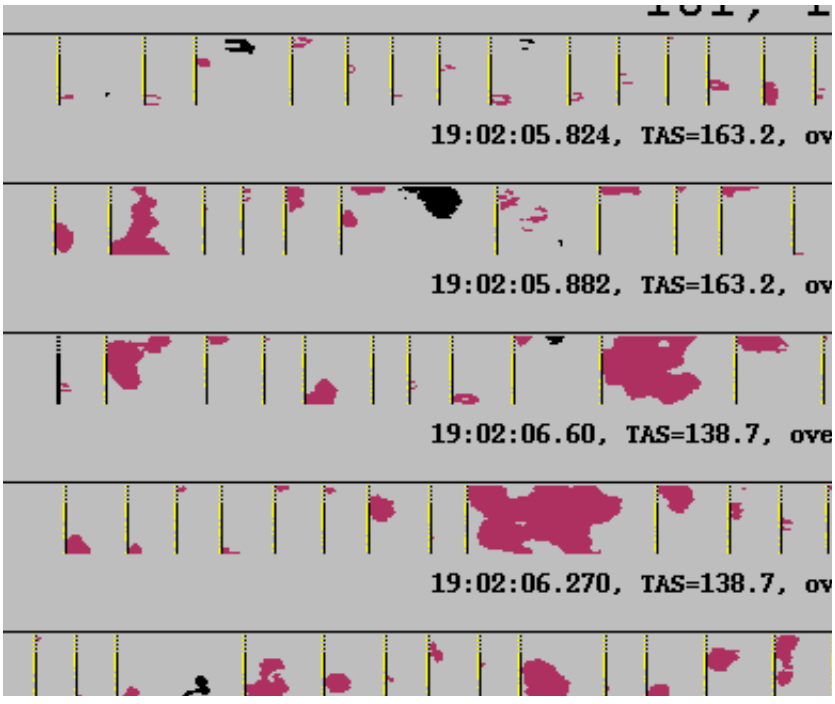

Instrument Description

Processing Description and Software

Data Acquisition Software

Data Formats

Data Catalog

Display/Analysis Software

Data Distribution

Summary Datasets

Return to Instrument List

PMS-2D Processing Software

Overview

For the most part data are distributed in raw format. Starting with DYCOMS-II in mid-2001, RAF will be producing 1D histograms from the 2D probes. Two sets of histograms will be produced. The "1DC" arrays will emulate the 260X ("Entire-in"). The "2DC" arrays will use a "Center-in" approach to reconstruction.

Definitions:

- h = height along the diode array.
- w = width along the flight path.

"1DC/P" Histograms ("Entire-in")

These histograms will emulate the 260X probe where particle size is determined as the maximum particle height. Rejection criteria are as follows:

- Reject particles which occlude either end diode.
- Reject particles with a height of zero (zero area images).
- Reject particles where h * 4 < w).

A particle is determined to end at the first blank slice encountered, this has the effect of shortening or removing many shattered particles.

The Sample Volume per bin per second is determined as follows:

2D-C:

Data processed prior to June of 2006 used the following DOF:

```
DepthOfField[i] = { 1.56, 6.25, 14.06,


DepthOfField[i] = { 61.0, 61.0, 61.0, .... 61.0
EffectiveAreaWidth[i] = 6.0 - (0.2 * i-1)
```

2D-P:

Instrument Description

Processing Description and Software

Data Acquisition Software

Data Formats

Data Catalog

Display/Analysis Software

Data Distribution

Summary Datasets

Return to Instrument List

PMS-2D Data Acquisition Software

Platform

VME system with custom interface card. Card plugs into ADS system.

Operating System

VxWorks 5.3.1

Language

C++

Instrument Description

Processing Description and Software

Data Acquisition Software

Data Formats

Data Catalog

Display/Analysis Software

Data Distribution

Summary Datasets

Return to Instrument List

PMS-2D Data Formats

The PMS2D raw data comes in 4 kilo-byte records of 32 bit slices from the probe (1024 slices). The interface card then wraps a record header around that with time stamp and other pertinant information. The Logical records are then packed 7 at a time into a "physical" record (orginally done to maximize tape speed and/or storage), this packing is not required.

The data is stored in **big-endian** format, so all data will need to be swapped when used on Intel architecture (Linux or MS Windows).

PMS-2D "Logical" Record Format

```
/* Possible values for the 'id' field. */
#define PMS2D_C1          0x4331          // First 2
#define PMS2D_C2          0x4332          // Second
#define PMS2D_G1          0x4731          // First 2
#define PMS2D_G2          0x4732          // Second
#define PMS2D_H1          0x4831          // First H
#define PMS2D_H2          0x4832          // Second
#define PMS2D_P1          0x5031          // First 2
#define PMS2D_P2          0x5032          // Second

struct P2d_rec {
  short id;                               /* 'P1','C
  short hour;
  short minute;
  short second;
  short spare1;
  short spare2;
  short spare3;
  short tas;                              /* true ai
  short msec;                             /* msec of
  short overld;                           /* overloa
  unsigned char data[4096];               /* image b
  };
typedef struct P2d_rec P2d_rec;
```

id

The `id` word tells whether it is a 2d-C, 2d-P or an HVPS. The 1 or 2 signifies first or second probe. Hex values are 'C1' = 0x4331, 'P1' = 0x5031 etc.

Time stamp

The `hour, minute, second`, and `msec` belong to the **LAST** slice of the record. This time stamp is stamped the moment the VME interface card is interrupted by the probe when a record is ready

Instrument Description

Processing Description and Software

Data Acquisition Software

Data Formats

Data Catalog

Display/Analysis Software

Data Distribution

Summary Datasets

Return to Instrument List

PMS-2D Display/Analysis Software

- Support Information
  - Supported Operating Systems
    - Unix/Linux
  - Programming Languages used
    - C++
  - Support Libraries and required tools
    - X11R5 with Motif 1.2 (OpenMotif) or later.

- Components
  - **xpms2d** - quick viewer.
  - **ncpp** - View quantitative data (histgrams, etc) produced from the nimbus 2d processor.

Instrument Description

Processing Description and Software

Data Acquisition Software

Data Formats

Data Catalog

Display/Analysis Software

Data Distribution

Summary Datasets

Return to Instrument List

PMS-2D Data Distribution

- Same as ADS data policy

Who gets access to the data; what does it cost?

- Same as ADS data policy

Available data format

- binary (tape image)
- stripped binary

FTP location

- www.eol.ucar.edu

Supported tape formats

- Binary
- Tar

Contact:
Who do I contact to obtain these data?

- RAF Data Manager (Ron Ruth)
- rafdmg at ucar.edu
- (303)497-1084

Last update: Tue Aug 24 12:29:02 MDT 1999

RAF Bulletin No. 24

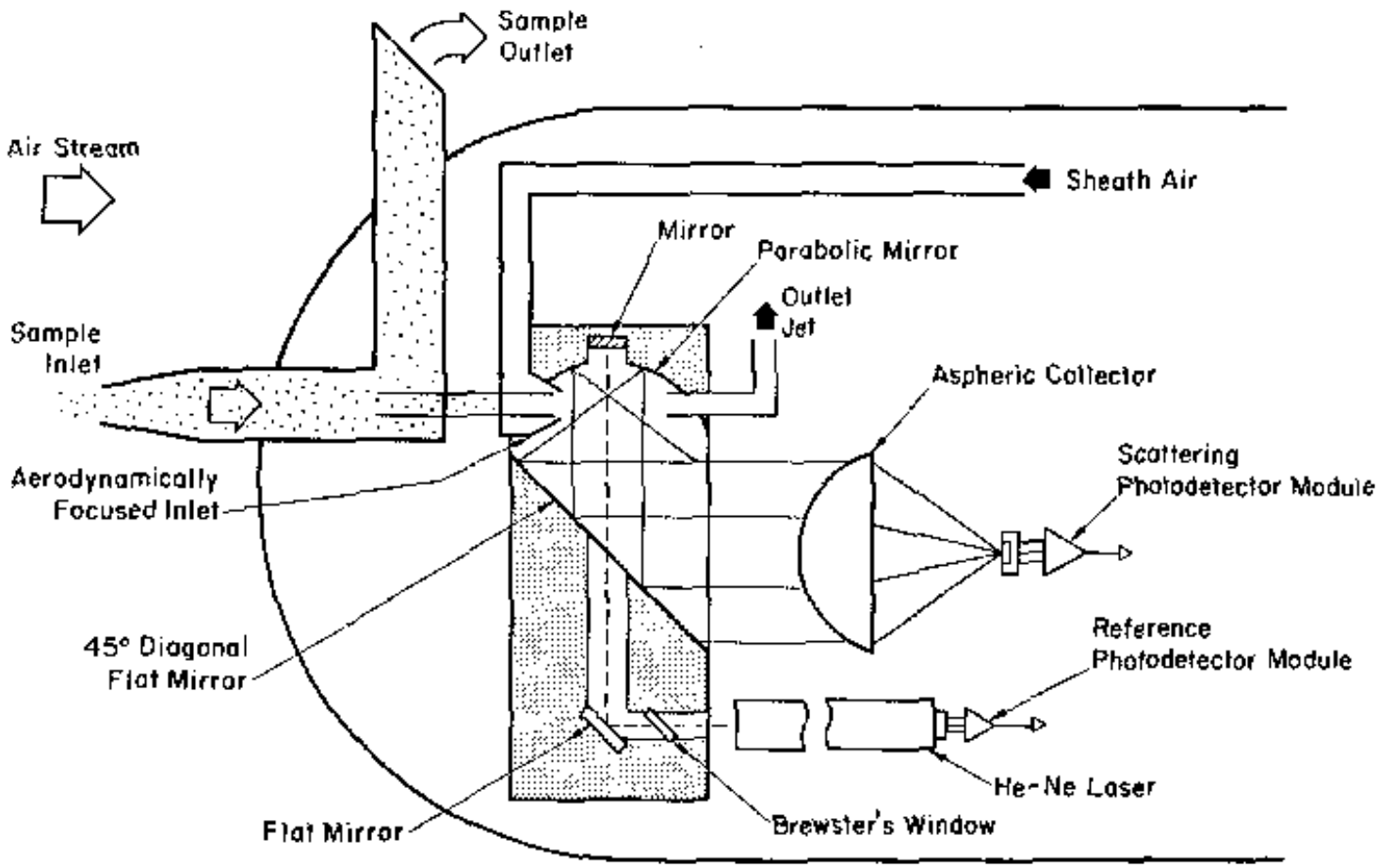

Figure 2. A schematic diagram of the ASASP's optical detection system

---

Last update: Wed Dec 6 13:40:39 MST 2000

RAF Bulletin No. 24

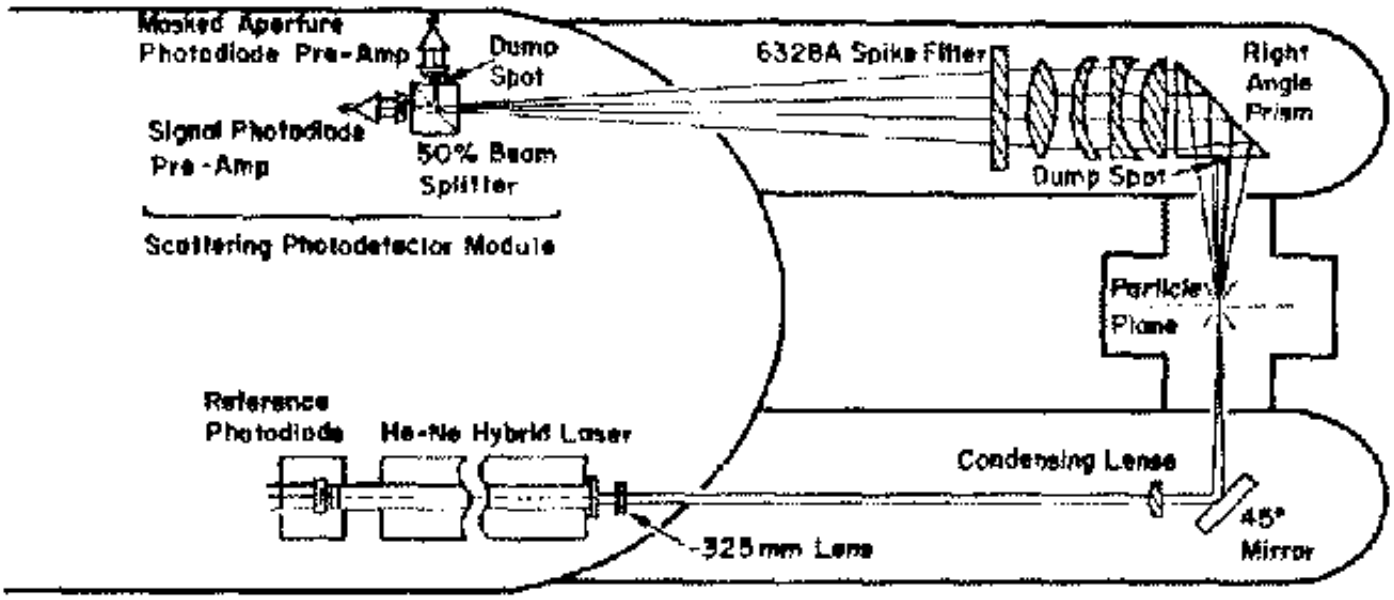

Figure 3. A schematic diagram of the FSSP's optical detection system

---

Last update: Wed Dec 6 13:40:48 MST 2000

RAF Bulletin No. 24

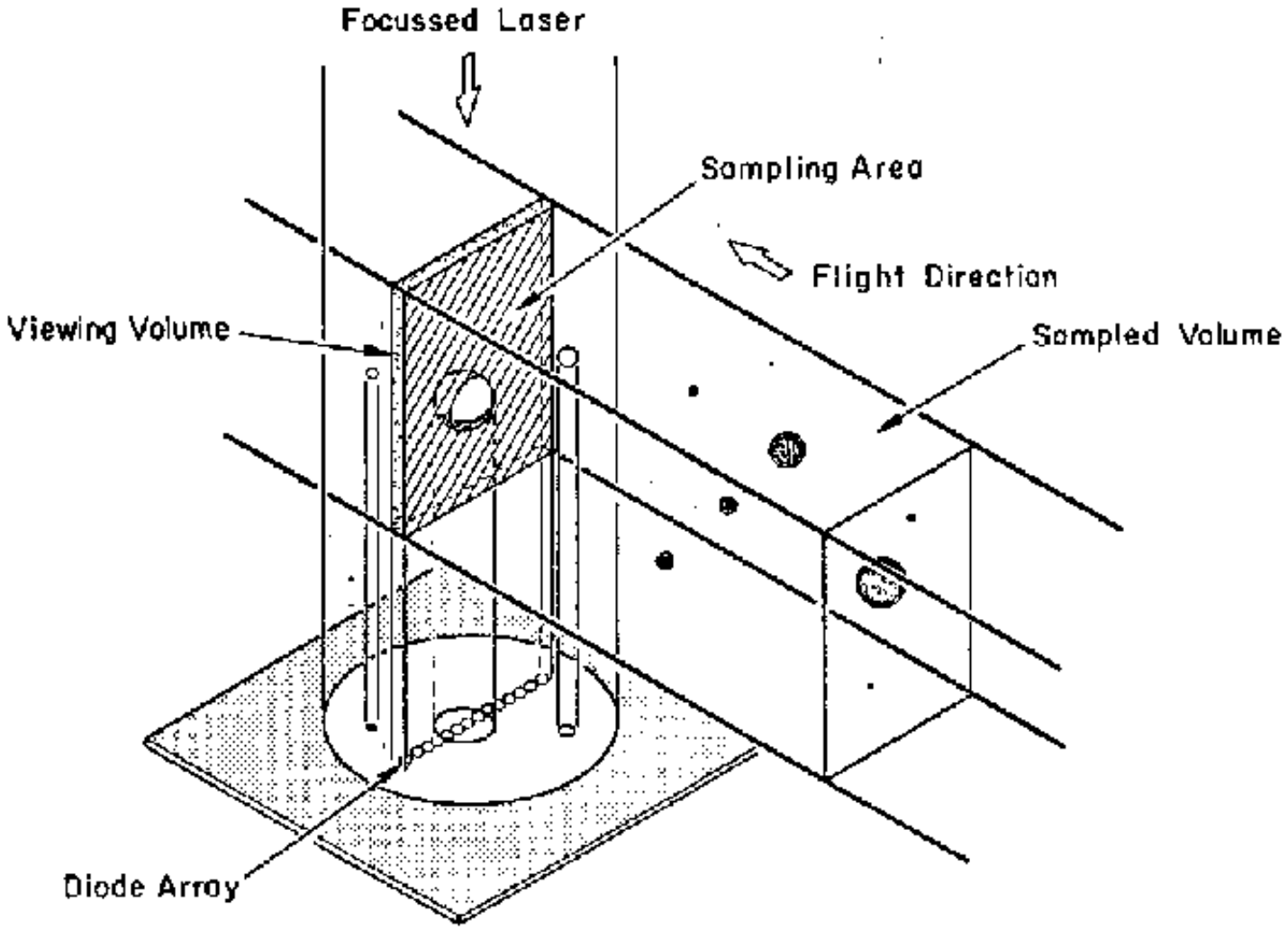

Figure 4. A graphical representation of the optical probe's imaging principles

---

Last update: Wed Dec 6 13:41:10 MST 2000

RAF Bulletin No. 24

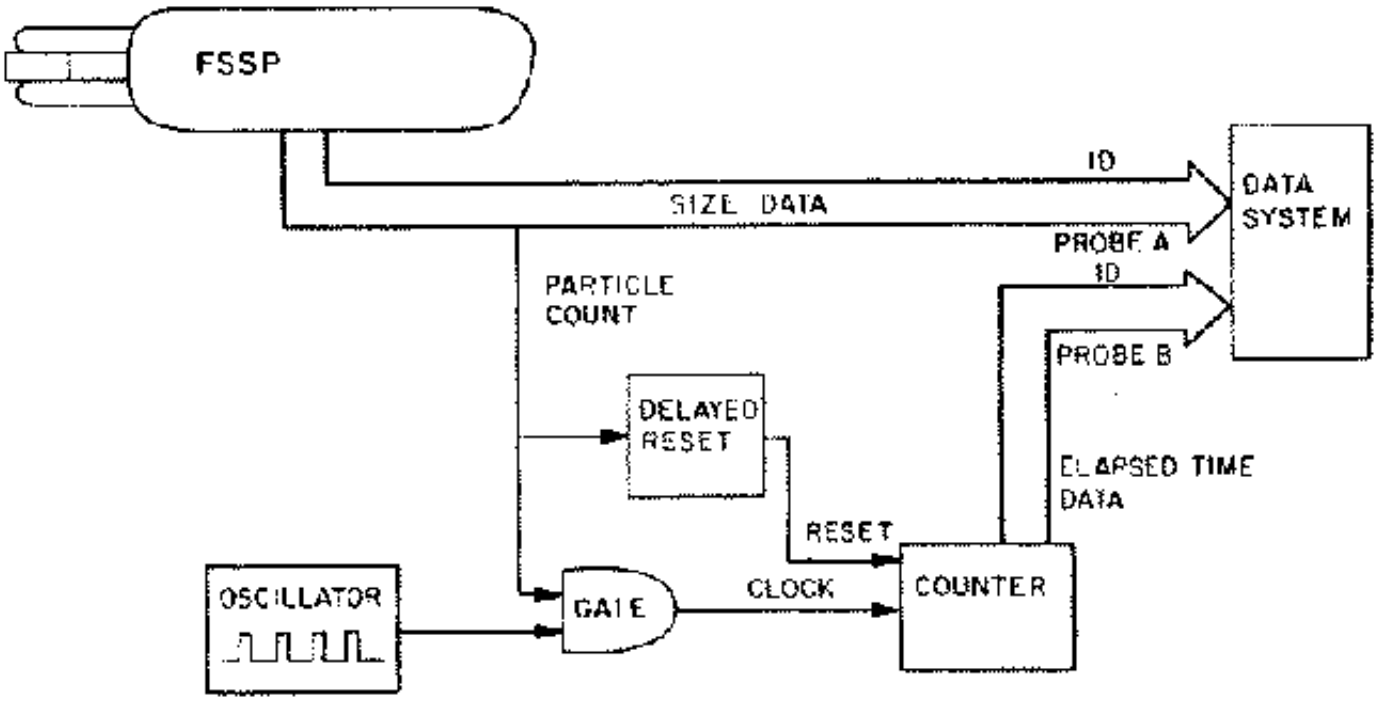

Figure 5a. Block diagram illustrating the PSM's operating principles

---

Last update: Wed Dec 6 13:41:26 MST 2000

RAF Bulletin No. 24

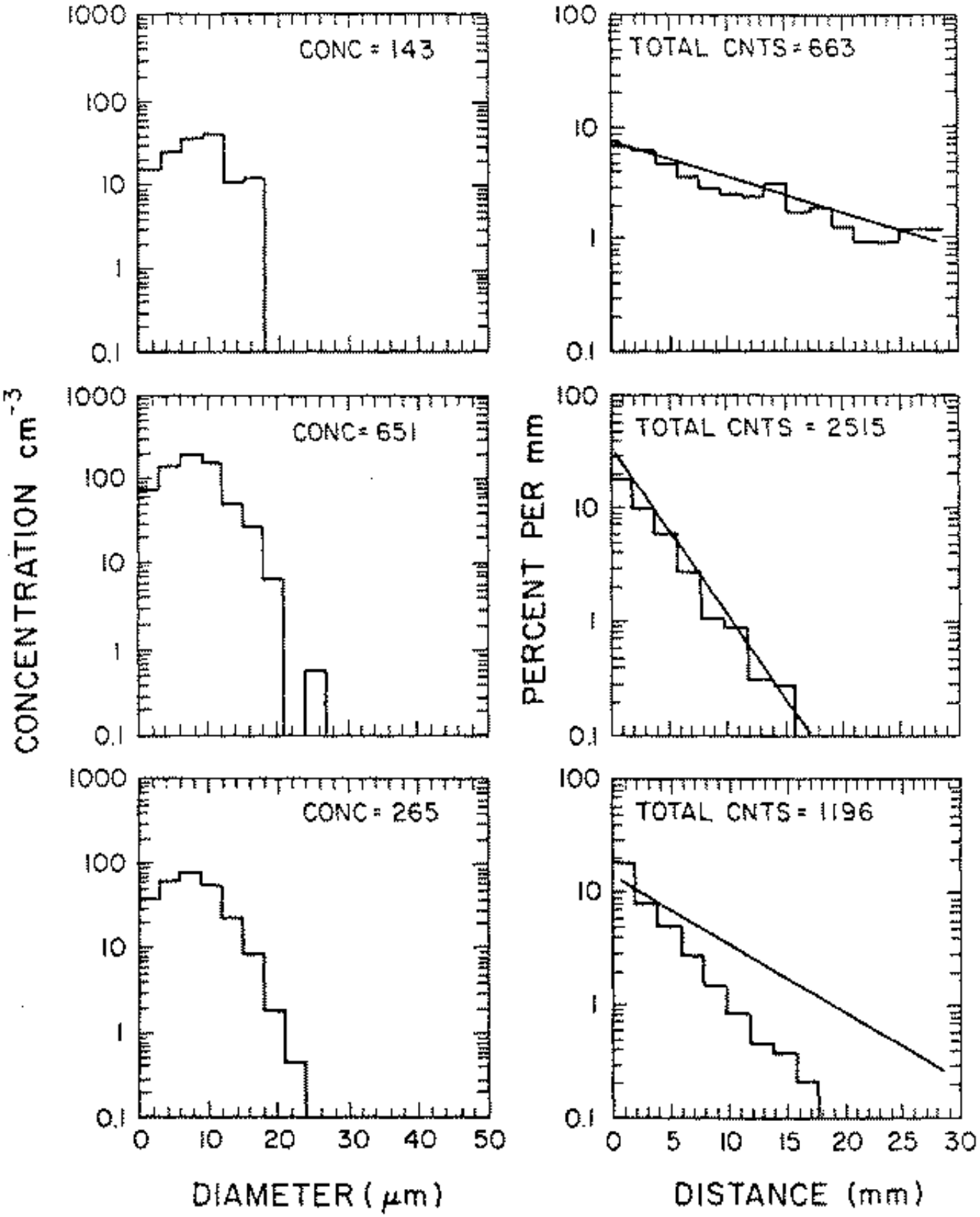

Figure 5b. An example of the measured time interval distribution of cloud droplets

Last update: Wed Dec 6 13:41:35 MST 2000

RAF Bulletin No. 24

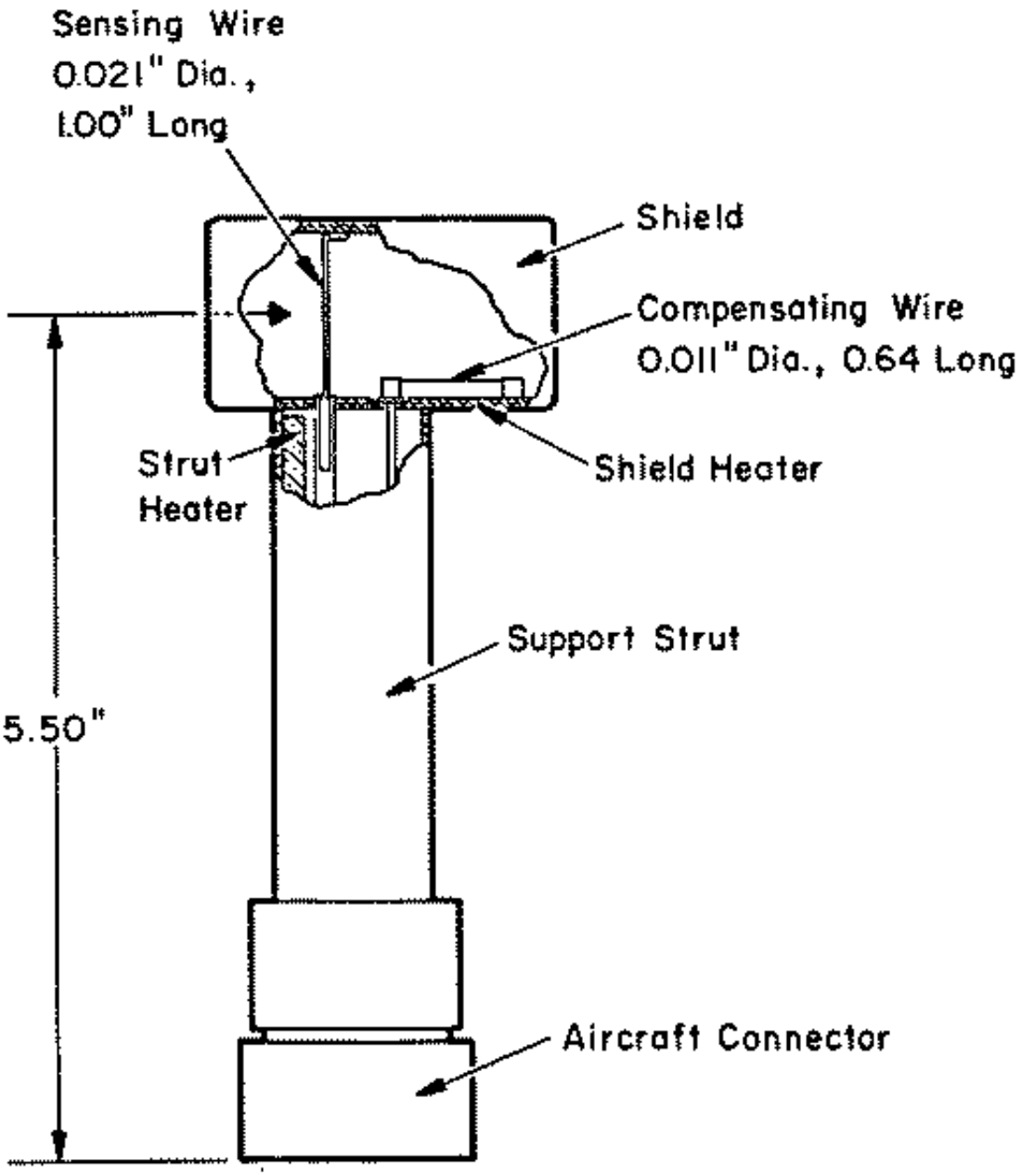

Figure 6a. Cross-sectional diagram of the Johnson-Williams probe

---

Last update: Wed Dec 6 13:41:50 MST 2000

RAF Bulletin No. 24

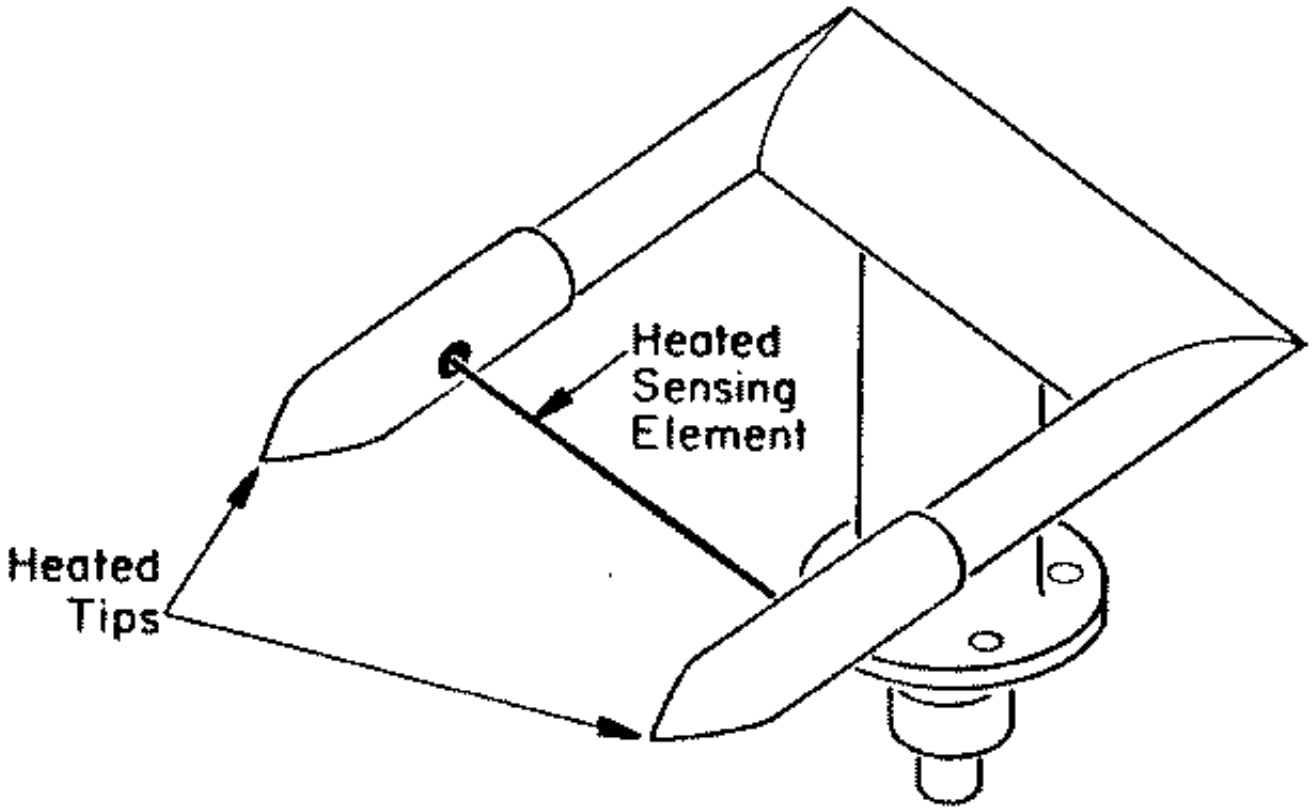

Figure 6b. Graphical illustration of the PMS/CSIRO (King) hot-wire probe

---

Last update: Wed Dec 6 13:42:01 MST 2000

RAF Bulletin No. 24

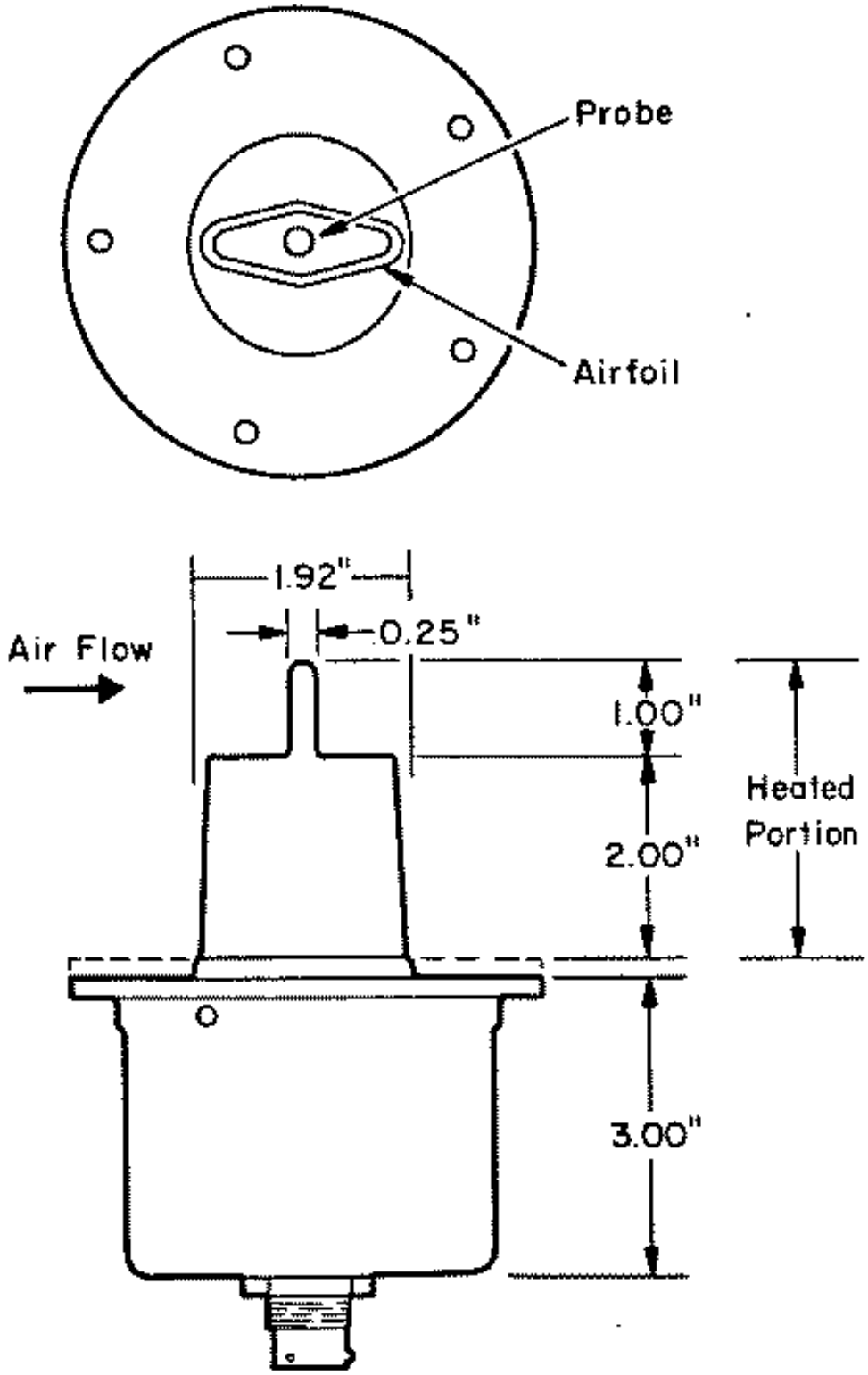

Figure 7. A schematic drawing of the Rosemount ice detector (reproduced from the Rosemount, Inc. ice detector operations manual)

Last update: Wed Dec 6 13:42:14 MST 2000

RAF Bulletin No. 24

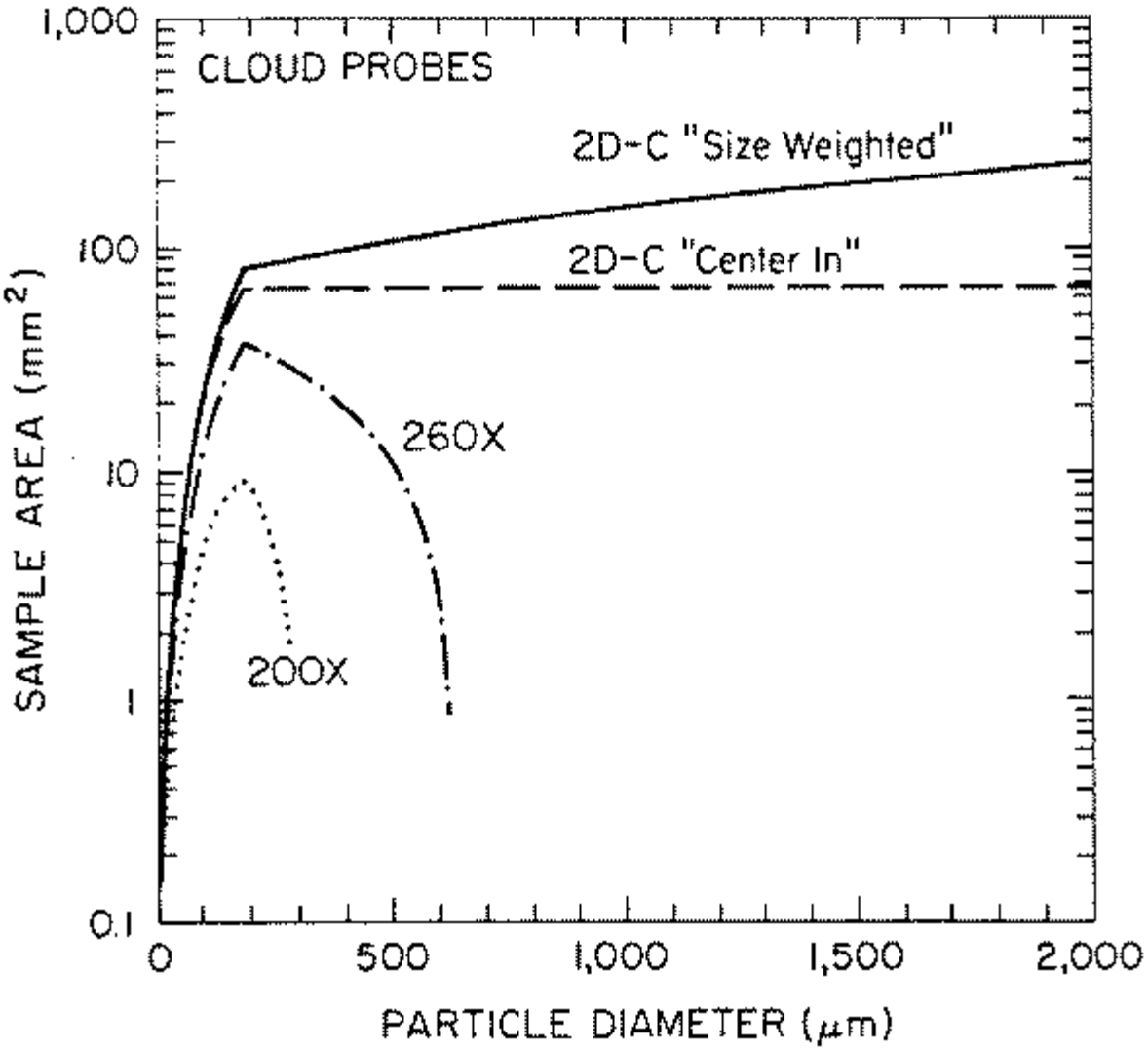

Figure A.1. The relationship between sample area and particle diameter for the three types of cloud droplet probes

---

Last update: Wed Dec 6 13:42:24 MST 2000

RAF Bulletin No. 24

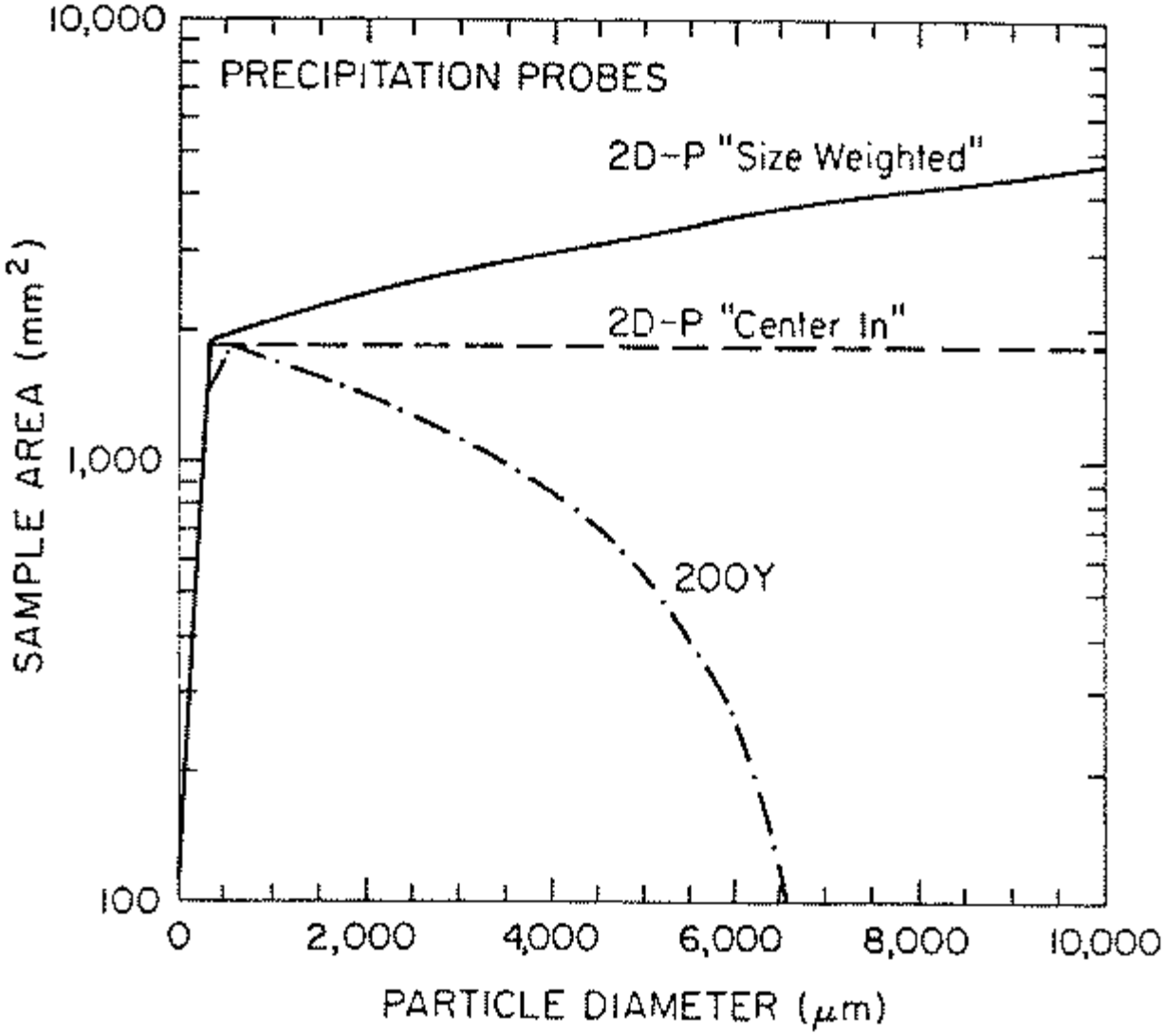

Figure A.2. The relationship between sample area and particle diameter for the two types of precipitation probes

---

Last update: Wed Dec 6 13:42:32 MST 2000

RAF Bulletin No. 24

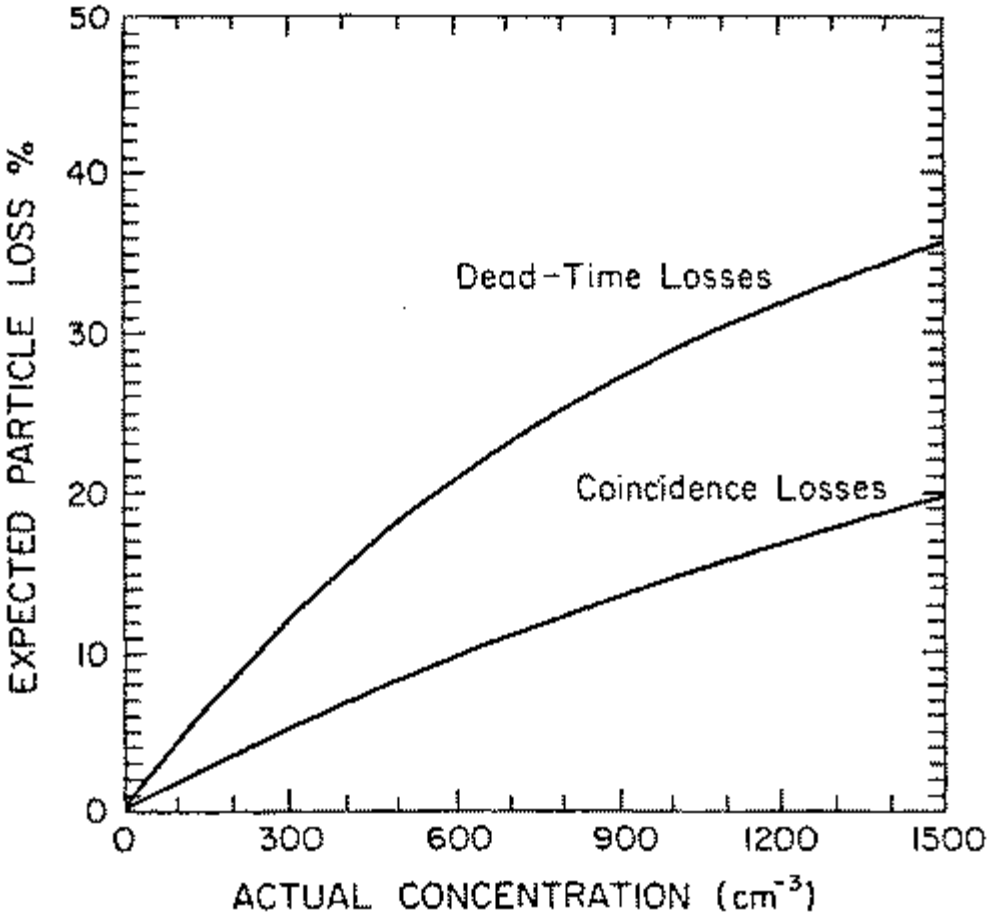

Figure B.1. This graph illustrates the magnitude of coincidence and dead-time losses as a function of concentration for the RAF FSSP flying at a speed of 100 M/s

---

Last update: Wed Dec 6 12:46:22 MST 2000

RAF Bulletin No. 24

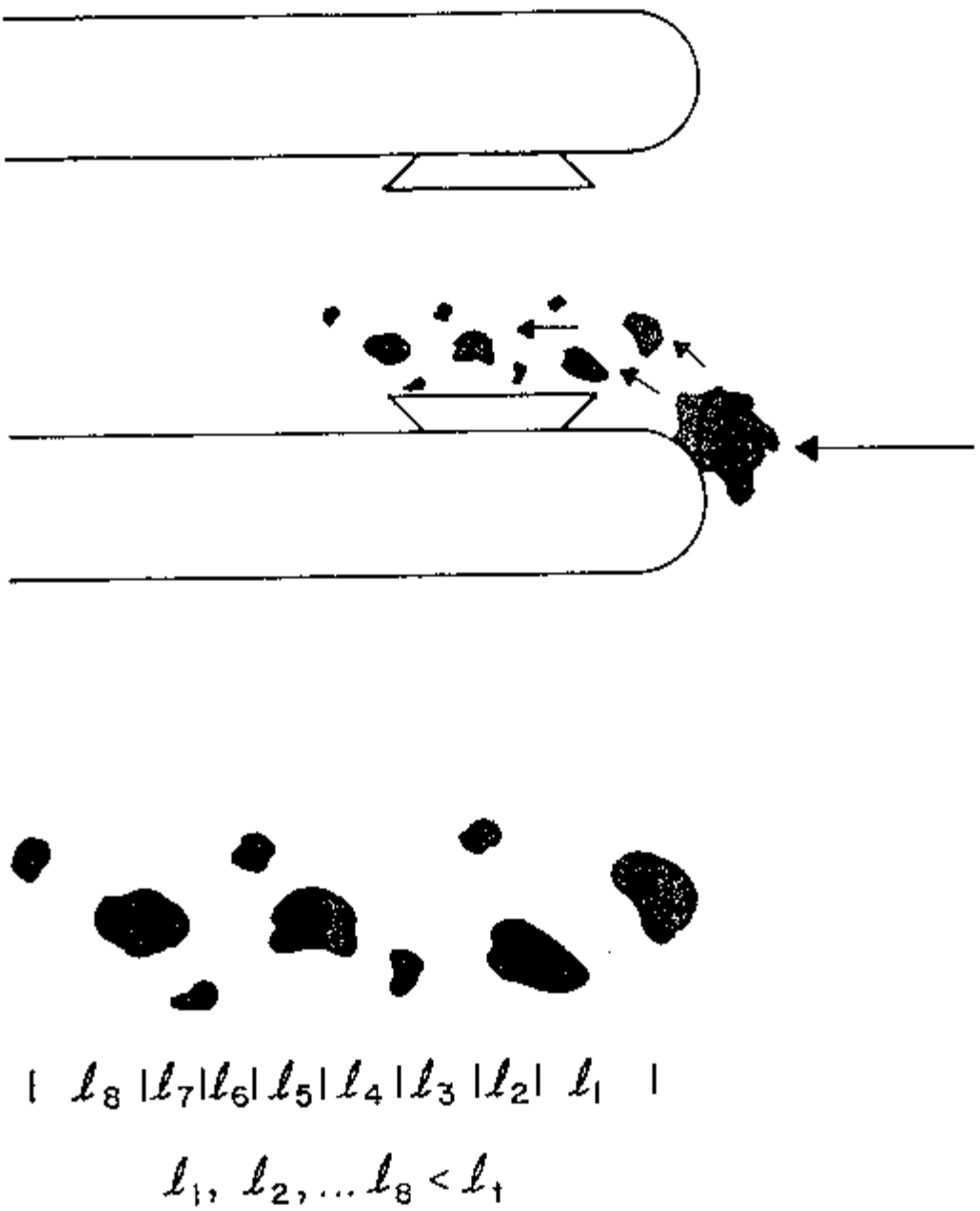

Figure D.1. Example of spurious particles generated by the breakup of a large particle on the probe tip

---

Last update: Wed Dec 6 12:30:16 MST 2000

RAF Bulletin No. 24

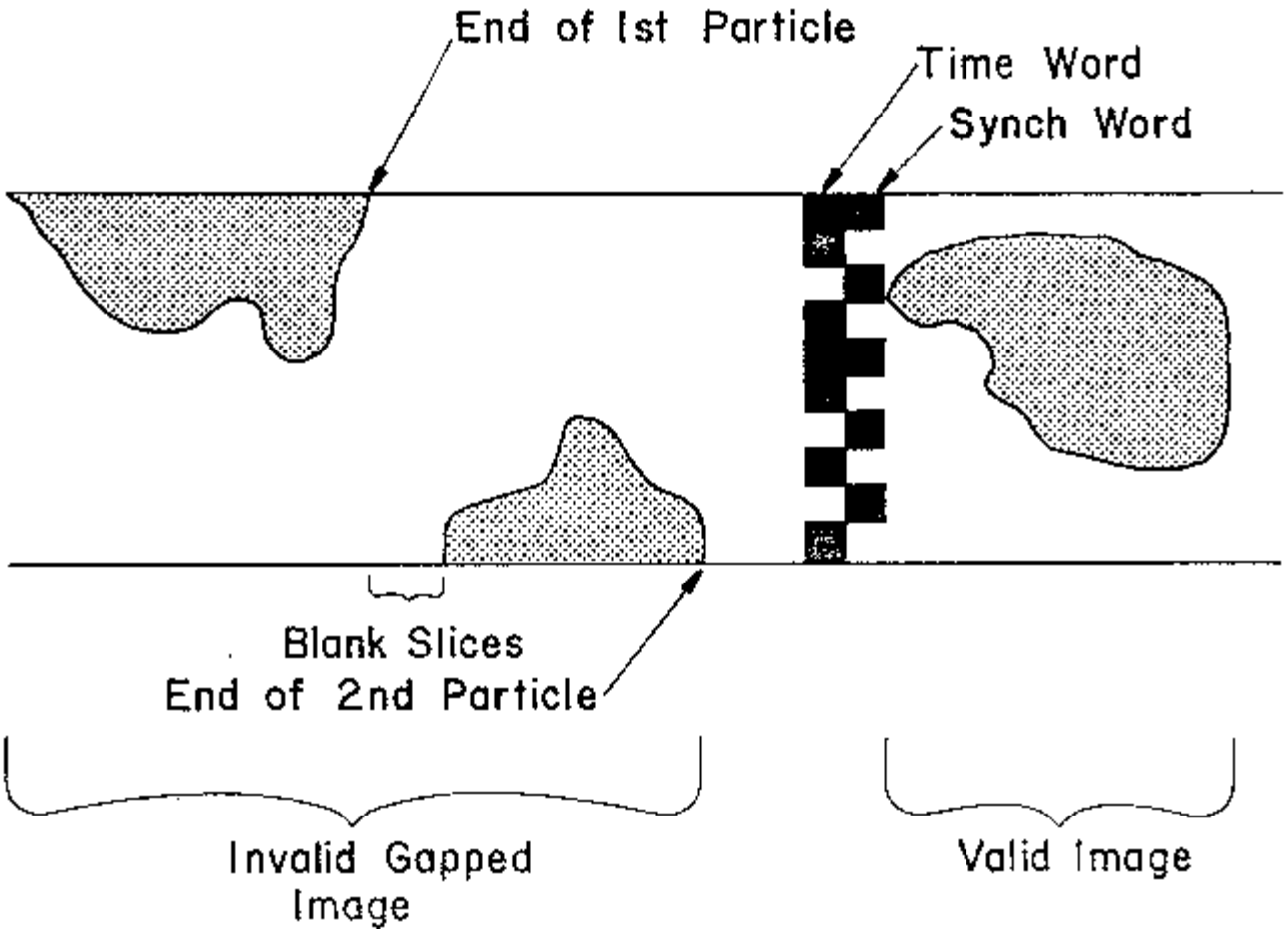

Figure D.2. Example of a gapped image

Last update: Wed Dec 6 12:30:52 MST 2000

RAF Bulletin No. 24

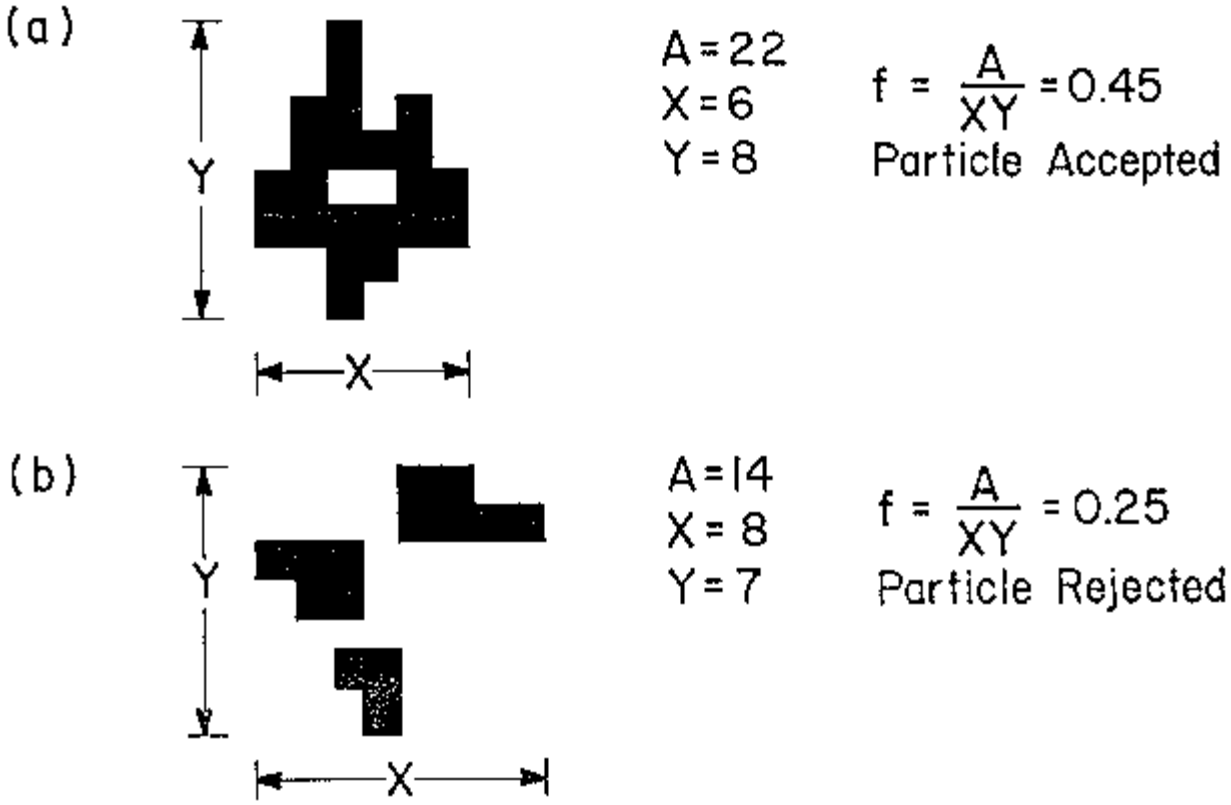

Figure D.3. Schematic representation of the algorithm used for rejecting hollow particles

---

Last update: Wed Dec 6 12:31:09 MST 2000

RAF Bulletin No. 24

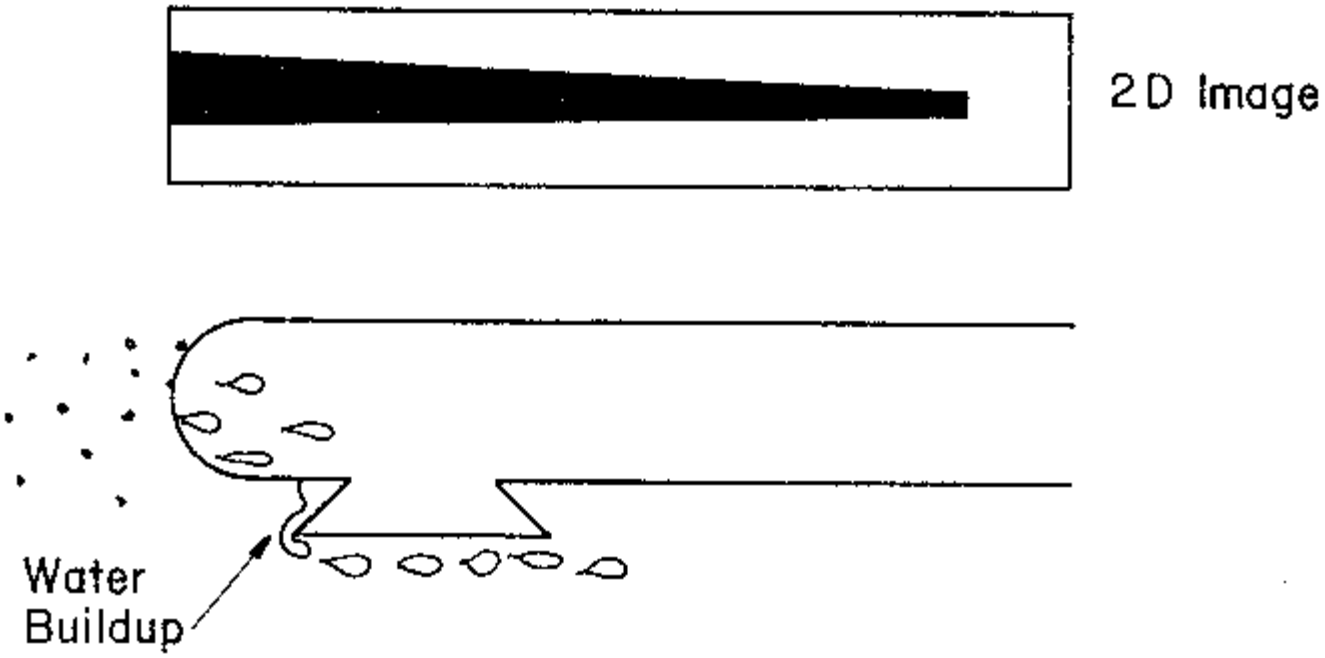

Figure D.4. A typical "streaker" image

Last update: Wed Dec 6 12:31:17 MST 2000